CHAPTER ONE

Introduction

1.1 Introduction:

The optic chiasm is an important landmark .It is a flattened quadrilateral x-shaped structure located at the bottom of the brain immediately below the hypothalamus, It receives the optic nerves by its anterior angles and emits the optic tracts by its posterior angles. (Barkovich AJ1989)

Several anatomic studies on cadaver specimens without intracranial pathology performed in the 20th century showed that about 80% of the optic chiasms overlie the diaphragm sellae, which are defined as normal in their position the remaining 20%were equally distributed between the prefixed variant (located above the tuberculin sellae) and the post fixed variant (situated superior to dorsum sellae) (Berglund Retal 1969).

When interpreting magnetic resonance (MR) examinations of the brain. The optic chiasm is formed by the union of the two optic nerves. The nasal fibers of each optic nerve decussate (cross) across the chiasm to the contralateral side while the temporal fibers course posteriorly to form the optic tract on the ipsilateral side. This arrangement allows the left half of the visual field to end up on the right side of the brain and the right half of the visual field to locate to the left side.

Several important structures are located adjacent to the optic chiasm. The supraclinoid branches of the internal carotid artery flank the chiasm. The cavernous sinuses are lateral and inferior to the chiasm. The frontal lobe of the brain lies above. The pituitary gland sits below in the sella turcica. The

sella turcica is bound in front by the tuberculum sellae and behind by the dorsum sellae. Behind the chiasm lies the floor of the third ventricle.

(Lee etal 2005)

A small chiasm can be an indication of several disorders, the most common of which is septooptic dysplasia, and a large chiasm can be the result of glioma, meningioma, lymphoma, or hemorrhage.

The diagnosis of atrophy or enlargement of the chiasm has largely been made by "gestalt" interpretation, and is therefore highly subjective and variable among observers. (Hupp SL 1991)

Magnetic resonance imaging (MRI) and computerized tomography (CT) have added a new dimension in the diagnosis and management of ocular and orbital diseases. Although CT is more widely used, MRI is the modality of choice in select conditions and can be complimentary to CT in certain situations. The diagnostic yield is best when the ophthalmologist and radiologist work together. Ophthalmologists should be able to interpret these complex imaging modalities as better clinical correlation is then possible. (Surv. 1991)

There have been several studies focus on the anatomy of the optic chiasm and anatomic variation of neurovascular structures adjacent to it using MRI, in Sudan there is no publications about optic chiasm measurements.

1.2 Problem of the study:

There are no specific characterization of the size and measurements of the normal optic chiasm or related changes due to age and gender in Sudan which could help in the early detection of some disorders.

1-3 Objectives:

1.3.1 General objectives

To study characteristics of optic chiasm dimensions in normal MRI brain.

1.3.2 Specific objectives:

- To measure the optic chiasm diameters (width& height) in coronal MRI Images.
- To compare the findings with clinical evidence of headache, visual disturbance, and optic atrophy.
- To correlate the findings with patient age, and gender
- To establish whether there was significant difference between abnormal MRI finding with the chiasm measurements.
- To use routine protocol of MRI brain as technique for measurement the optic chiasm diameters (width& height).

1.4 Over view of study:

To make the aims of the project stated above true, an attempt is made to back up the practical work, which is the ultimate aim of this research, by the theoretical background. This is described through the chapters of the thesis in a sequential manner. In chapter one a summarized introduction including prelude about brain lesions, objectives, hypotheses, and over view of chapters contents were present. In chapter two an over view of the literature including anatomy, physiology and pathology of the brain were included. Imaging methods also took place as well as the previous studies and theoretical back ground as it is an important point of this research.

Chapter three dealt with the material used in the practical study including different imaging modalities machines, Also the methodology of the practical setup was discussed in details.

Chapter four dealt with the results of the study.

The results interpretations are giving in this chapter. Also given in chapter five are the conclusions of the study performed as well as future prospect and recommendations.

CHAPTER TWO

Theoretical Background

The optic chiasm is formed when the optic nerves come together in order to allow for the crossing of fibers from the nasal retina to the optic tract on the other side. This enables vision from one side of both the eyes to be appreciated by the occipital cortex of the opposite side. This review makes note of the embryology, anatomy and vascular supply of the optic chiasm, then discusses the clinical syndromes associated with chiasmal disease, and the diseases which commonly influence its function. (Wiley 2014)

2-1 Embryology

The anlage of the structure of optic chiasm is seen initially within the floor of the third ventricle at around three weeks of gestation, rostral to the hypophysial duct and between the optic stalks, at the junction of telencephalon and diencephalon. Nerve fibers develop and it dissociates itself forwards from the ventricle. Fibers from the optic nerves reach the chiasm between the 4th and 6th weeks (Barber et al., 1954) and crossed and uncrossed fibers can be seen by the 11th week; hemidecussation of fibers is completed by the 13th week. It assumes its characteristic shape by the 15th week, when the eyes have moved from a lateral to a more anterior position. (Meissirel et al, 1994)

2-2 Anatomy

The chiasm lies above the sphenoid bone, over the diaphragm sellae (Fig. 2-1); anatomical variations are common and can influence the presenting visual symptoms and signs in chiasmal disorders. In the majority of cases, the chiasm is situated overlying the diaphragmasellae, pre- fixed when lying above the tuberculum sellae or within the sulcus chiasmatis (17% of cases), and post fixed when it lies above or even behind the dorsum sellae (4%) (Bergland et al., 1968). (Kidd, D2011).

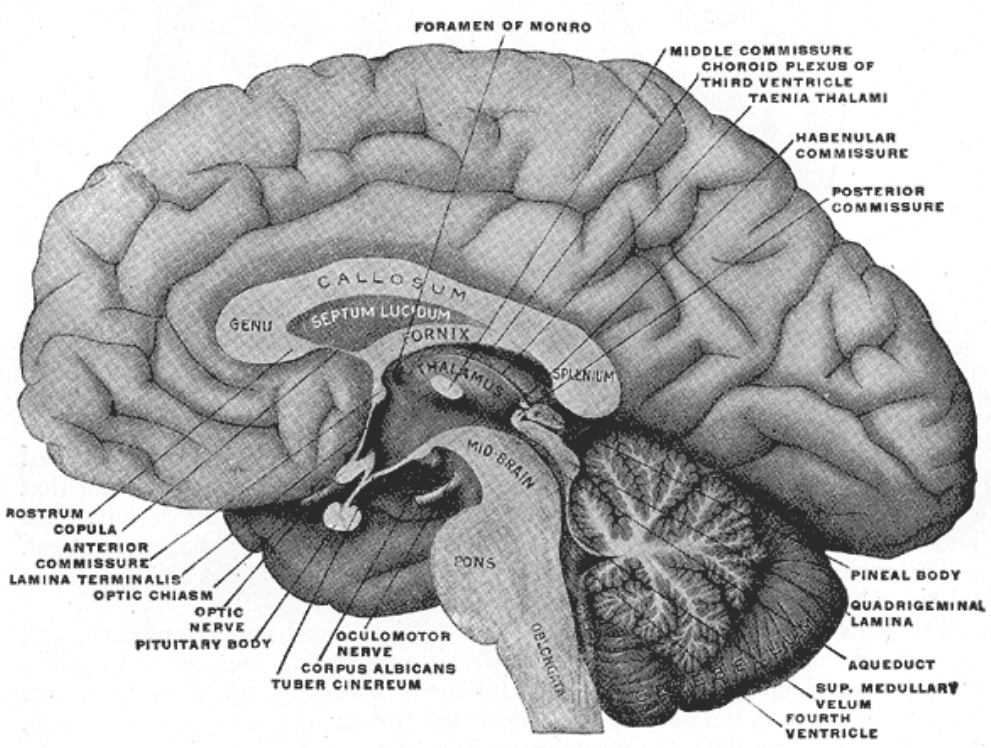

Figure (2.1) shows the optic chiasm in a brain sectioned in the median sagittal plane

. The intracranial optic nerves rise from the canal to the chiasm at an angle of 15–45°. The pia mater is contiguous with that of the nerves and that of the anterior tracts. The chiasm lies posterior superiorly within the wall of the third ventricle and anteriorly with the CSF within the chiasmatic cistern (Fig. 2-1). Above lies the hypothalamus, bounded by the lamina terminalis which itself forms the anterior wall of the third ventricle. The chiasm invaginates the ventricle, so separating the optic recess above and the infundibular recess below. Below the chiasm lie the sellaturcica, the pituitary gland, and the diaphragmasellae. It is separated from these structures by the basal cistern. Here too there are variations which may influence the visual disorders arising from disease within these structures; the width of the cistern, the shape of the pituitary gland, and the size of the diaphragmasellae all influence what size a lesion must attain before compression of the chiasm occurs.

The infundibulum of the pituitary lies immediately posterior and the mammillary bodies behind this, medial to the two optic tracts. (fig2.2)

The internal carotid arteries as they emerge from the cavernous sinuses lie to either side, and the anterior communicating artery lies directly above; aneurysms of the anterior communicating artery or first segment of anterior cerebral artery may therefore compress the chiasm. (Kupfer, 1967).

Over two million nerve fibers pass through the optic chiasm from the eyes; fibers from the nasal retina cross; the ratio of crossed to uncrossed fibers within the chiasm is 53:47 This crossing is of necessity very precise; only fibers from the temporal retina pass to the ipsilateral lateral geniculate nucleus, and only those from the nasal retina pass contra laterally. Those

which cross do so as soon as they enter the chiasm and maintain their rostral to caudal position within. Those which are uncrossed continue in the lateral chiasm into the ipsilateral tract. Fibers from the macula on each side which account for the majority of fibers within the chiasm (Hoyt et al, 1963) are found more centrally and caudally than other fibers.

Rarely the chiasm may fail to develop (achiasmia). Patients studied have associated midline developmental disorders but intact fields; the visual evoked potential characteristically is monocular (Sami, 2005).

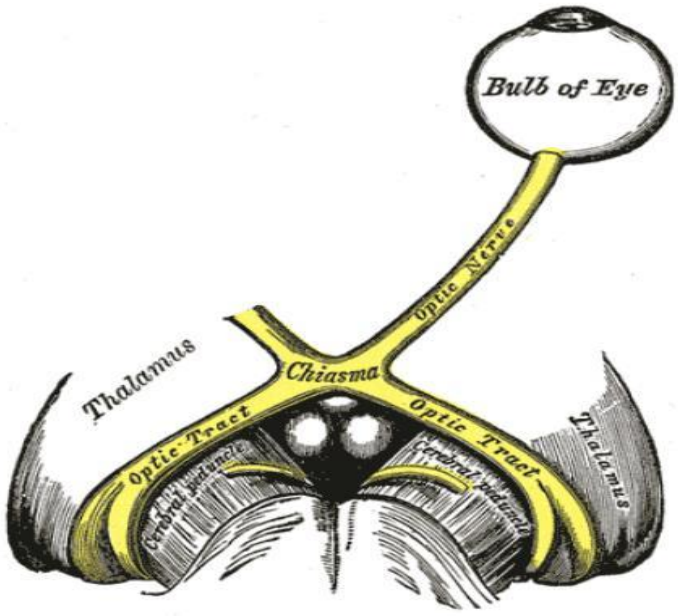

(Fig2.2) shows the optic chiasm

2.2.1 Blood supply

The blood supply is variable, but in general comes from feeder vessels arising from branches of the anterior communicating artery, anterior cerebral, posterior communicating, posterior cerebral, and basilar arteries the dorsal parts are supplied by branches of the ICA and the more ventral parts from the posterior circulation. There is considerable collateral supply; hence infarction of the chiasm is very rare indeed. (Wollschlaeger et al., 1971).

2.3 Physiology of optic chiasm:

In binocular organisms, retinal ganglion cell (RGC) axons from the nasal hemiretina generally cross the brain midline and project to their visual targets in the contralateral brain hemisphere, the lateral geniculate nucleus (LGN) and the superior colliculus. However, some fibers from the temporal retina do not cross the midline but rather they project to targets on the same side. This axonal hemidecussation takes place at the ventral diencephalon midline, in a structure known as the optic chiasm. The main function of the optic chiasm is to organize the inputs from the same point in the visual field perceived by each retina, directing these to the same location in the visual cortex. It is there, in the visual cortex, that the two subtly different images are integrated into cohesive three-dimensional representation, (Eloisa 2008)

2.4 Pathology of the Optic Chiasm:

There are a number of disorders than can affect the optic chiasm. These include: inflammatory disorders such as multiple sclerosis, infections such as tuberculosis, benign (non-cancerous) tumors and cysts, cancerous tumors, vascular (blood vessel) disorders.

The most common disorder affecting the optic chiasm is a pituitary adenoma. Pituitary adenomas are benign tumors. In most cases, they have no impact at all, but in some cases, they can affect vision, sometimes causing vision loss. As they grow in size, pituitary adenomas can put pressure on important structures in the body, such as the optic nerve. Putting pressure on the optic nerve may cause blindness, so it is crucial for eye doctors to detect pituitary tumors before they cause damage to vision. The pituitary gland is about the size of a bean and is attached to the base of the brain behind the nasal area. It sits right under the optic chiasm. Although small, the pituitary controls the secretion of many different types of hormones. It helps maintain growth and development and regulates many different glands, organs, and hormones. Changes in hormones can cause significant changes in our bodies. Besides vision changes such as double vision, drooping eyelids, and visual field loss, (kidd D 2011)

Pituitary adenomas also may cause the following symptoms :(Forehead headaches, Nausea or vomiting, Change in sense of smell, Sexual dysfunction, Depression, Unexplained weight changes, Change in menses or early menopause

Why Diseases of the Optic Chiasm May Be Hard to Detect When a disease or lesion affects the optic nerve before it reaches the optic chiasm in the brain, the defect in the vision will show up in only one eye and can affect the entire field of that eye. People that suffer from a one-sided defect sometimes do not notice it until one eye is covered. This is because, when both eyes are open, the overlapping visual fields of each eye will mask the defect. If the disease affects the optic tract after the chiasm, the person will have a defect

in their vision in both eyes, but the defect will alter the same half of the visual field. (Sashank 2016)

2.4.1 Visual field defects in chiasmal disorders

A careful study of the bilateral visual field defect acquired in chiasmal lesions can provide important information on the nature and in particular the site of the causative lesion. Traditionally, field defects have been divided anatomically into the anterior angle, the body, the posterior angle, and the lateral aspect of the chiasm.

2-4-1.1 The Anterior Angle

Lesions which involve the anterior angle of the chiasm, the point at which the optic nerve passes into and forms the chiasm, may show a junctional scotoma since there is at this point separation of the crossing and uncrossed fibers. If the lesion is not large this will result in an ipsilateral monocular central field defect (from the optic nerve) and a small contra lateral upper temporal homonymous field defect from involvement of the crossing fibers anteriorly If the nerve itself is not affected as well, then the defect will be monocular and temporal, since only the crossing fibers are affected; if only the macular fibers are involved then the defect is a midline obeying temporal scotoma This defect may be very small and can be missed with kinetic perimetry; it is usually picked up using static perimetry, however. (Traquair, 1949)

Wilbrand's knee is said to be an extension of the crossing fibers from retinal ganglion cells located nasal and inferior to the fovea into the ipsilateral distal optic nerve; the contra lateral field defect arising with involvement of these.

however, has stated that Wilbrand identified an art factual state in examination of enucleated eyes. Nonetheless, the identification of a small asymptomatic contra lateral defect in the presence of a symptomatic monocular defect should encourage the examining physician to proceed with haste to imaging studies rather than diagnosing an inflammatory optic neuropathy incorrectly. (Horton (1977),

2-4-1.2 The Body of the Chiasm

Lesions which affect the body of the chiasm produce the typical bitemporal hemianopia this may affect the whole hemifield, upper or lower quadrants and peripheral or central areas (fig2.3). The macula is usually but not always split. In general, central visual acuity is unaffected. Clearly, it is possible that the field defects are not the same in each eye, since the causative lesion may exert a greater effect on one side than the other. Complete defects tend only to occur in the case of trauma. When the peripheral fields are affected, the defect progresses in a clockwise direction in the right and anti-clockwise in the left Lesions compressing from above cause the lower field to be affected first and the defects are less congruous; those from below affect the upper fields first and tend to be more congruous in appearance. (Walker, 1915).

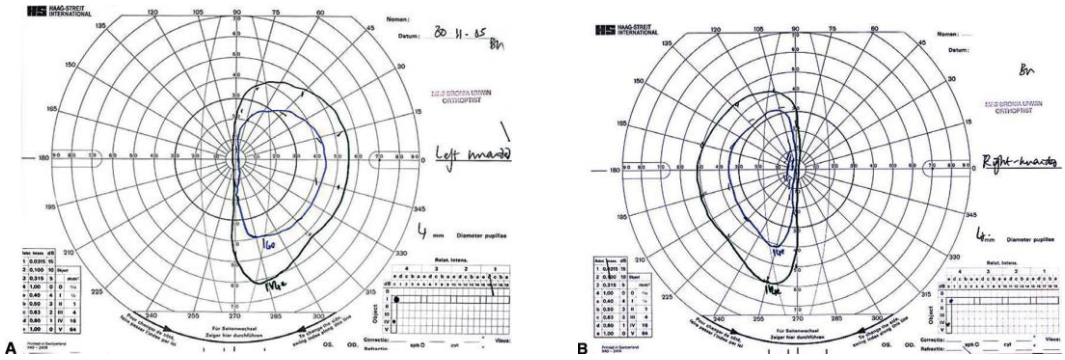

Fig (2-3): Goldman field showing bitemporal hemianopia caused by a lesion involving the body of the chiasm. (Cushing and Walker, 1915).

2-4-1.3 The Posterior Angle of the Chiasm

Lesions within the posterior aspect of the body of the chiasm produce bitemporalhemianopic scotomas These may be confused with centrocaecal scotomas (Fig. 2.4), but the former will not be associated with significant reduction in visual acuity whereas the latter will. (Larmonde, 1977).

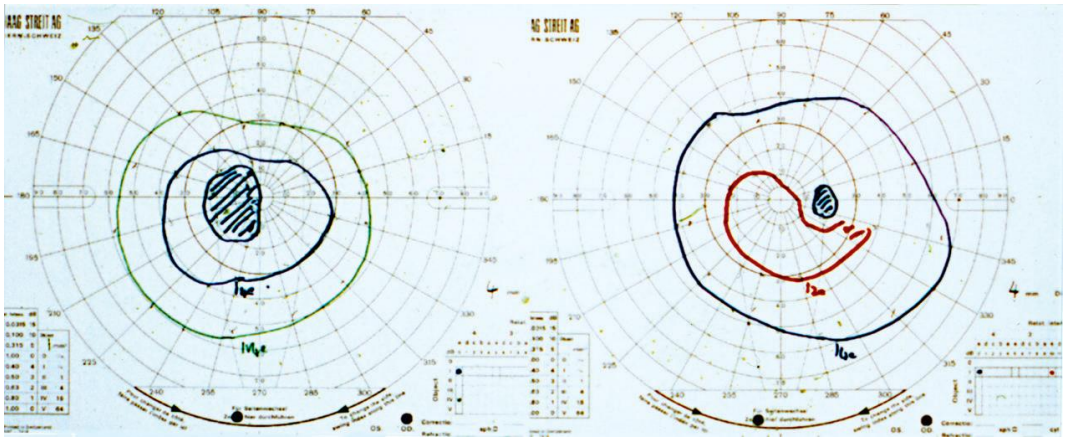

Fig (2-4): Goldman field showing a field defect associated with a lesion involving the posterior angle of the chiasm. (Larmande et al, 1977)

More posterior placed lesions will also involve the optic tract, with the results that the field defected will be predominately one of a homonymous hemifield defect.

2-4-1.4 The Lateral Aspect of the Chiasm

Involvement of this region by compression leads to a homonymous hemifield defect on the contra lateral side (Fig. 2-4).

2.4.1.5 Visual Symptoms

When lesions damage chiasmal fibers, there is a progressive loss of central visual acuity and a noticeable dimming of the temporal visual fields.

Patients may also notice a disturbance of depth perception at fixation which is due to crossing of the two blind hemi fields after the point of fixation in convergence. Hence an object seen at a distance to be behind another will disappear when the eyes focus on the one in front. “Hemifield slide” causes difficulty in reading in which the patient notices a doubling, loss or vertical deviation of words on a horizontal line. Normally there is an overlap between the temporal field on one side and the nasal field on the other to allow fusion, which helps to stabilize ocular alignment, with the result that the image is clear. Patients with minor phoric deviations of the eyes will lose this overlap and therefore develop tropia (strabismus), with the result that minor horizontal or vertical misalignment occurs, leading to distortion or even doubling. Those whose lesions involve not only the chiasm but also the cavernous sinus or orbital apex may also have IV–VI neuropathies leading to diplopia and trigeminal sensory loss or pain. Some patients with chiasmal syndromes may rarely complain of photophobia; the mechanism by which this comes about is not clear. (Larmonde, 1977).

2.4.1.6 Neuro- Ophthalmic Signs

When a chiasmal lesion leads to optic nerve fiber atrophy "band" or "bowtie" atrophy is seen, in which atrophy is more evident in the nasal and temporal sides of the disc and relatively spared from the superior and inferior sectors (Fig. 2-5).This is due to involvement of only those fibers arising nasal to the fovea (associated therefore with the bitemporal hemianopia) being affected and passing into the nerve from these sections of the disc. (Unsold et al, 1980)

Fig (2-5) Photographs of the optic fundus showing bowtie atrophy of both discs in a patient with a large chromophobe adenoma of the pituitary gland. (Unsold et al, 1980)

Seesaw nystagmus; when vestibular fibers associated with the interstitial nucleus of Cajal are involved in tumors of the diencephalon and parasellar region a rhythmic synchronous alternating rotation of the eyes, in which one elevates and intorts whilst the other simultaneously depresses and extorts may arise. It is exceedingly rare (Leigh et al, 1991).

Sarcoidosis is an auto inflammatory disorder of uncertain aetiology in which granulomatous inflammation develops leading to tissue destruction and fibrosis. It is thought that some 10% of cases arise within or also involve the central nervous system. The neurological disorder is a meningeal based inflammatory infiltration (Kidd et al, 2003). The anterior visual pathway may be involved at any region (Frohman et al., 2003) ;(Koszman et al., 2008), or an optic per neuritis may arise. Involvement of the chiasm comes about by the development of an inflammatory mass within the pituitary gland (Guoth et al., 1998) (Fig. 2-6). Patients present with symptoms of hypopituitarism and with visual field defects in keeping with a chiasmal problem.

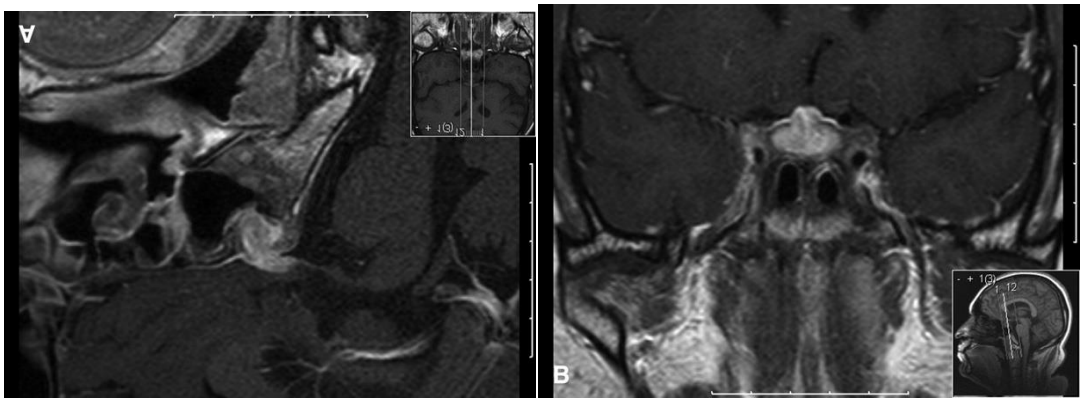

Fig (2-6): T1 weighted sagittal& coronal MRI showing enhancement of the hypothalamus and pituitary stalk in Sarcoidosis. (Frohman et al., 2003); (Koszman et al., 2008)

2-4.2 **Inflammatory Diseases** (**ANCA positive vasculitis**)

ANCA positive vasculitis is a granulomatous inflammatory disorder with features of arteriolar and venularperivasculitis which affects the lungs, skin, eyes, and kidneys. Neurological involvement arises as a hypertrophic pachymeningitis, as an isolated inflammatory mass or as a central or

peripheral manifestation of inflammatory perivasculitis (Seror et al., 2006). Most cases with pituitary involvement present with diabetes insipidus and not with a mass lesion (Yung et al., 2008), although the pituitary stalk may be thickened. Visual impairment is uncommon.

2-4.3 Lymphocytic infiltration

It is well known that the chiasm may be involved in multiple sclerosis (Beck et al., 1983); (Newman et al., 1991); in which chiasmal type field defects are seen in a sub-acute unilateral or bilateral visual loss typical of an optic neuritis. MRI shows swelling and oftentimes enhancement of the chiasm.

Idiopathic optic chiasmitis may be diagnosed when other infective and inflammatory causes have been out ruled. One series (Kawasakiet al, 2009) described 20 patients, 60% of whom were female, 40% presented with monocular visual loss but with evidence for chiasmal field defects, the remainder showing bitemporal hemianopia. MRI scans revealed chiasmal swelling with or without enhancement in 12/15 cases, and white matter lesions were seen elsewhere in 6/15 cases. Over time around half develop multiple sclerosis. An optic chiasmitis has also occasionally been seen in other systemic inflammatory diseases, for example, systemic lupus erythematosis and sarcoidosis. (Frohman et al., 2001).

2-4.4 Lymphocytic Hypophysitis

This uncommon condition is more common in women (by a factor of 5:1) and often occurs in the late stages of pregnancy or the early postpartum period (Kidd et al., 2003). Patients present with headache then signs of an expanding sellar lesion with visual impairment and endocrine hypo function. Many have other organ specific autoimmune diseases. Hypopituitarism arises

as a consequence of immune mediated attack on the pituitary cells, rather than simply a compressive effect. MRI shows a symmetrical intensely enhancing tissue mass within the pituitary and there may be a dural tail (Sato et al., 1998). The pathology of the lesion is one of intense infiltration by lymphocytes and plasma cells, often with lymphoid follicles, associated with evidence for necrosis of adjacent pituitary tissue. Antipituitary antibodies may be detected (Bensing et al., 2007) although the assays appear not yet to have clinical utility (De Bellis et al., 2008).

2-4-5 Histiocytic Infiltration

These conditions are rare; Xanthomatoushypophysitis is thought to be an incomplete form of the systemic disorder Erdheim Chester disease and RosaiDorfman syndrome presents with large often multiple inflammatory masses resembling meningiomas on MRI (Kidd et al., 2006).

2-4.6 Tuberculosis

Pituitary hypo function and visual field defects may arise as a result of the development of tuberculoma within the pituitary, giving rise to a mass lesion with chiasmal compression (Domingues et al., 2002) (Fig. 2.7) or to optochiasmalarachnoiditis, in which a basal tuberculous meningitis encroaches upon that region and induces visual loss, frequently in association with diabetes insipidus (Akhadder et al., 2001). Pituitary tuberculomas are indistinguishable from other mass lesions on MRI, although some say that thickening of the pituitary stalk is more common in TB. In optochiasmaticarachnoiditis imaging, there is perichiasmal enhancement (Silverman et al., 1995).

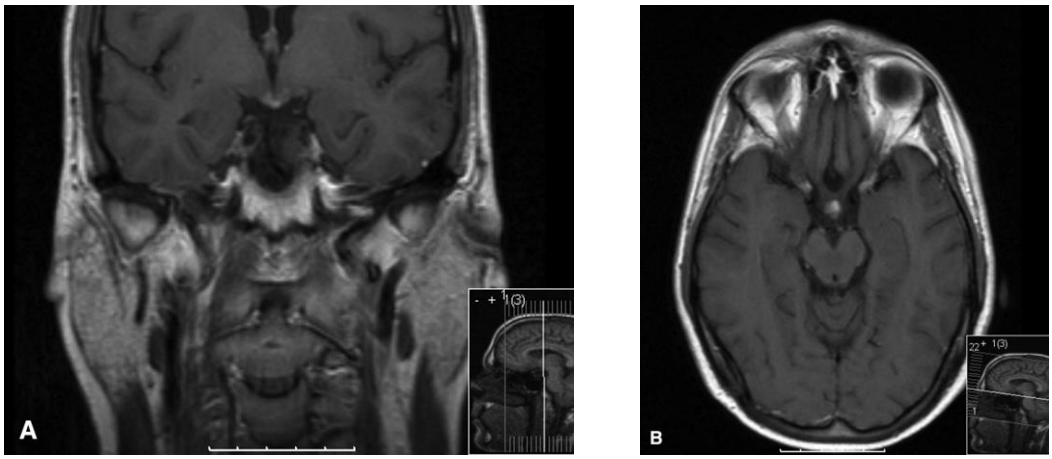

Fig (2-7): T1 weighted coronal& axial MRI showing enlargement and enhancement of the pituitary gland and stalk in tuberculosis. (Frohman et al., 2003) ;(Koszman et al., 2008

2-4.7 Pituitary abscess

One recent series noted that patients with abscesses present not with signs of fever or meningitis but with headache and visual loss mimicking a pituitary mass; most cases were only diagnosed at surgery when a pus filled mass was opened (Vates et al., 2001). Of 25 cases reported within the past 5 years around half grew no organisms, whilst the majority of the remainder were pyogenic organisms, fungi, or parasites (Dalan et al, 2008).

2-4.8 Cryptococcus

Optic neuropathy is common in cryptococcal meningitis; a pathological study showed that the nerves and chiasm were damaged as a result of direct infiltration by the organism from the adjacent meninges The prognosis for visual recovery even with prompt treatment is very poor. (Cohen et al, 1993).

2-4.9 Cysticercosis

Cases in which there was compression from the third ventricle onto the chiasm or intrasellar cysts causing compression from below have been reported (Chang et al, 2001).

2-4.10 Viruses

Isolated chiasmitis related to viral infections seems rare, but has been reported with VZV and EBV (Purvin et al., 1988); (Greven et al., 2001). It is more common to occur alongside a severe syndrome in which the uveal tract, retina and optic nerve, and chiasm may all simultaneously be affected (Brazis et al, 2005).

2-4.11 Tumors and Cysts

2-4-11.1 Pituitary adenoma

These constitute 10% of all intracranial tumors; the prevalence increases with age. Adenomas arise from tissues within the anterior pituitary; functioning or secreting adenomas secrete prolactin, somatotrophin, ACTH, and TSH. Most are microadenomas (measuring less than 10 mm in diameter and the majority will therefore present with the effects of hormone hypersecretion or as incidental findings. Non- secreting adenomas account for only 10% of cases but are more likely to be large, and present with visual loss and headache (Wilson, 1992) (Fig. 2.8).

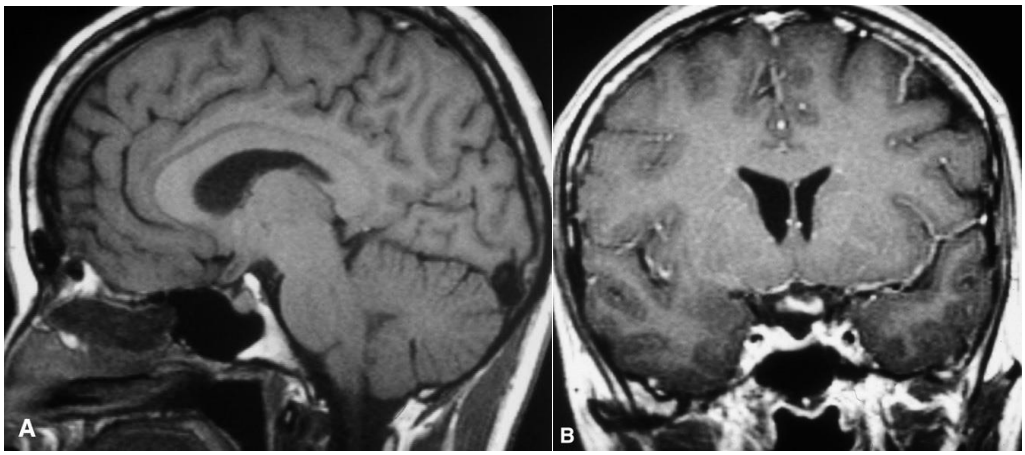

Fig (2-8): Pituitary adenoma: T1 weighted axial & coronal MRI showing a large chromophobe adenoma with cystic change causing chiasmal compression. (Newman et al., 1991)

Prolactinomas account for 40% of pituitary tumors and present with galactorrhea and amenorrhoea; the majority (90%) are microadenomas sdxsdx4ewwa (Schlechte, 2003). Corticothroph and somatotroph secreting tumors produce Cushing's disease and acromegaly/giantism, respectively. TSH secreting tumors are rarer.

2-4.11.2 Craniopharyngioma

These are benign lesions which nonetheless can cause prominent and irreversible pituitary and hypothalamic dysfunction. They arise from squamous epithelium at the junction of the infundibular stem and the anterior pituitary and are thought to be remnants of Rathke's pouch. There is a bimodal incidence, in childhood and again in middle to late life, with clinical features of a sellar or hypothalamic lesion. They may be situated above or below the chiasm, and rarely within it (Brodsky et al., 1988). The lesions are cystic (Fig. 2.9) and often contain viscid, oily (“engine oil”) fluid. Cholesterol clefts, calcium and keratin may also be present.

Fig (2-9): Craniopharyngioma: T1 weighted coronal MRI showing a cystic suprasellar lesion arising above and behind the chiasm. (Kidd et al., 2006)

In children, these lesions present with hypothalamic dysfunction and hydrocephalus; in adults, with features of chiasmal dysfunction, optic nerve or tract signs, and ophthalmoparesis.

2-4.11-3 Rathke's cleft cyst

These benign cysts form in embryogenesis if the lumen of Rathke's pouch does not close, giving rise to a cyst situated between the anterior and intermediate lobes of the pituitary. Most are asymptomatic and do not enlarge. Patients with symptoms are predominately female and present in middle life with visual loss due to chiasmal compression, headache, and hypopituitarism .It is difficult to diagnose with certainty on MR; there are features of craniopharyngioma or pituitary adenoma, and the diagnosis is usually made at surgery. (Voelker et al., 1991).

Epidermoid cysts in this region present with visual loss and hypothalamic dysfunction They are lined by stratified squamous epithelium; enlargement occurs due to progressive exfoliation from the epithelium of keratinous material which is laid down in a lamellar pattern. The rate of growth of these lesions is exceedingly slow. (Mtanda et al., 1986).

2-4.11-4 Choristomas in the sellar region

Dermoid cysts are also rare and similar to epidermoids except that the cyst is lined by pilosebaceous structures leading to the formation of hair. Whilst epidermoids are often laterally placed, dermoids tend to arise in midline structures. Rupture of these cysts is associated with chemical meningitis and seizures; those in the suprasellar region may therefore present with an apoplectic disorder similar to pituitary adenomas. Occasionally cystic lesions also arise in the optic nerve, chiasm, or tract. The lesions are found to be composed of muscle and adipose tissue (Zimmerman et al., 1983).

2-4.11.5 Suprasellar arachnoid cysts

These arise relatively frequently and present with signs of compression of the underlying structures, but occasionally upwards leading to hypothalamic dysfunction and hydrocephalus. It is difficult with imaging to differentiate these from other cystic lesions such as Rathke's cleft cyst and the diagnosis is often only made at surgery; treatment is with incision and fenestration of the cyst with a low risk of recurrence. (Rao et al., 2008).

2-4.11.-6 Chordoma

During development of the axial skeleton the notochord is compressed and sequestration occurs but notochordal remnants may persist into life. Most are

found in the sacrococcygeal region but some 25% arise in the base of the skull Here they arise most commonly from the clivus, where they present with diplopia due to sixth nerve paresis, but extension upwards may lead to optic tract or chiasmalinvolvement and hypothalamic dysfunction. The prognosis depends on the histological appearances, but in general these are slow growing lesions. (Stippler et al., 2009).

2-4.11-7 Germinoma

These uncommon tumors of early adult life arise most commonly in the pineal region but may also be seen in the suprasellar region, where they may arise from the floor of the third ventricle or from the chiasm itself. Those in the sellar region present with visual failure and hypothalamic dysfunction, particularly diabetes insipidus. Germinomas are locally invasive and may metastasise. (Tageuchi et al., 1978)

Other germ cell tumors such as teratoma and yolk sac tumors are rare and response to treatment is usually very poor.

2-4.11.-8 Glioma

Gliomas may involve the chiasm either by arising within the chiasm itself or by infiltration from the hypothalamus. They show similar histological features to those of unilateral optic nerve gliomas, and may also arise in neurofibromatosis. They may present at any age but are more common in children. The onset of visual loss is usually insidious, and may even be discovered at a routine checkup. The discs are usually pale at presentation, and the field defects bitemporal (Dutton, 1994). Headache may also be a feature. Imaging shows enlargement of the chiasm, sometimes with cysts and rarely with calcification (Hoyt et al., 1987). Treatment is more often

hazardous than helpful; the long- term visual prognosis is overall fair (Cappelli et al., 1998).

Malignant optic nerve glioma may also affect the chiasm. This presents with a much more rapidly evolving clinical syndrome and responds poorly to treatment (Rudd et al., 1985). Metastasis to other parts of the nervous system may arise (Murphy et al., 2003). The pathology of the lesion is very different to that of the benign chiasmal glioma, and is more similar to that of glioblastoma multiforme (Hamilton et al., 1973).

2-4.11-9 Meningioma

These tumors are twice as common in women as men and arise more frequently in the second half of life. They tend to be benign and slow growing but some may infiltrate the underlying tissues. The chiasm may be affected by those which arise from the sphenoid wing, the clivus, and the olfactory groove (Cockerham et al., 2005), and primary optic nerve sheath meningiomas may grow backwards to involve the chiasm. Tuberculum sellae or parasellarmeningiomas are uncommon (Fig. 2-10), accounting for some 3% of intracranial meningiomas. (Dutton, 1992) ;(Miller, 2008)

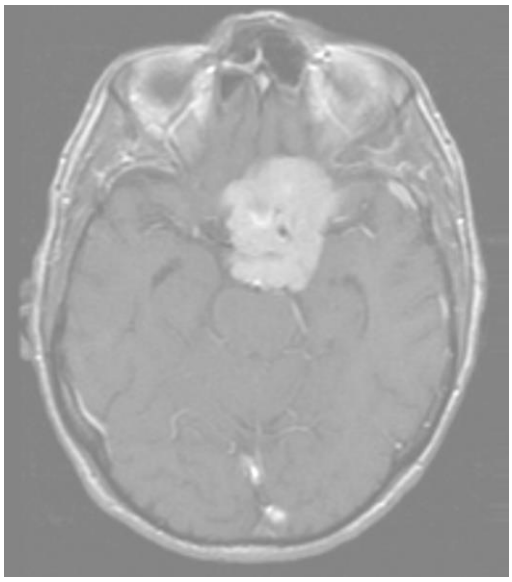

Fig (2-10): Meningioma: T1 weighted axial MRI showing a medial sphenoid ridge meningioma extending onto the lateral body of the chiasm. (Hughes et al., 2008),

2-4.11-10 Metastatic tumors

Metastasis to the sellar region has been reported with most carcinomas and lymphoreticular cancers. (Cockerham et al., 2005)

2-4.12 Vascular Disorders

2-4.12-1 Cavernoma

The majority present acutely with visual loss due to bleeding. A total of 87% of one series who underwent surgery showed an improvement in visual acuity post- operatively (Crocker et al., 2008).

Arteriovenous malformations may rarely arise within the chiasm and provoke a variety of syndromes, including transient bilateral visual obscurations, and field defects due to bleeding (Sibony et al., 1982).

2-4.12-2 Ischemia

The extensive blood supply to the chiasm has been noted above and for this reason ischaemic infarction of the chiasm is exceedingly rare.

2-4.12-3 Compression from Hydrocephalus

A host of visual field defects has been seen in hydrocephalus, due to compression of the optic nerve, chiasm, and tract When the third ventricle presses downwards directly and symmetrically onto the chiasm, a bitemporal hemianopia or upper quadrantinopia would be expected (Fig. 2.11). (Brazis et al, 2005).

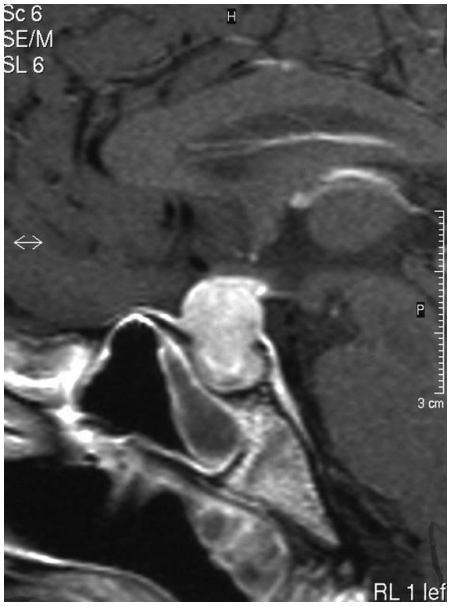

Fig (2-11): Chiasmal compression from downwards displacement of the third ventricle in hydrocephalus due to obstruction by a lesion of the tegmentum. (Brazis et al, 2005).

2-4.13 Traumatic Chiasmal Syndromes

These usually develop in victims of motor accidents and are associated with skull and facial fractures. The field defect is a complete bitemporal hemianopia. In one series, the prevalence of associated diabetes insipidus was 37% (Hassan et al., 2002).

2-5 Fundamentals of MR1

Magnetic resonance images are created by the application of energy to excitable tissues in a powerful static magnetic field via radio frequency pulses.Various pulse sequences are employed to differentiate between tissue types, and the ophthalmologist should have some familiarity with their nomenclature and use. Spin echo is the most commonly used sequence employing a set of two pulses. Repetition time (TR) is the time between pulse sets. Echo time (TE) is defined as the interval between the initial pulse and when the receiver coils "listen" for an echo. By altering the TR and TE values .Gadolinium-diethylene triamene pentacetic acid (Gd-DPTA) is an intravenous contrast agent. Because of its paramagnetic properties Gd-DTPA enhances, structures on T1-weighted images that have an incomplete or absent blood/brain barrier or slow blood flow (e.g., cavernous sinus).

2-5.1 Brain MRI technique:

In order to imaging the optic chiasm and intra-cranial optic pathways we usually use brain MRI with special slice cuts fig(2.12) , (Westbrook, 2008).

2-5.2Common brain MRI indications:

Multiple sclerosis, Primary tumor assessment and/ or metastatic disease, Infarction, Hemorrhage, Hearing loss, Visual disturbance, Infection, Trauma Unexplained neurological symptoms.

2.5-3 Equipment:

Head coil fig (2.13), Immobilization pads & straps, Ear plugs, High performance gradient for EPI, diffusion, and perfusion imaging

2-5-4 Patient positioning

The patient lies supine on the examination couch with their head with in the head coil. Use cushion & straps to immobilization the patient's head, Place cushion under the knees to take pressure off the back.

Plug the coil to the scanner and press aligned on to activate the positioning light. Ask the patient to close his/her eyes during the scan.

The patient is positioned so that the longitudinal alignment light lies in the midline, and the horizontal alignment light passes through the nasion. Multislice coronal images were prescribed. On the basis of midline sagittal section centering on appoints 3 mm anterior to the pituitary stalk (Westbrook, 2008).

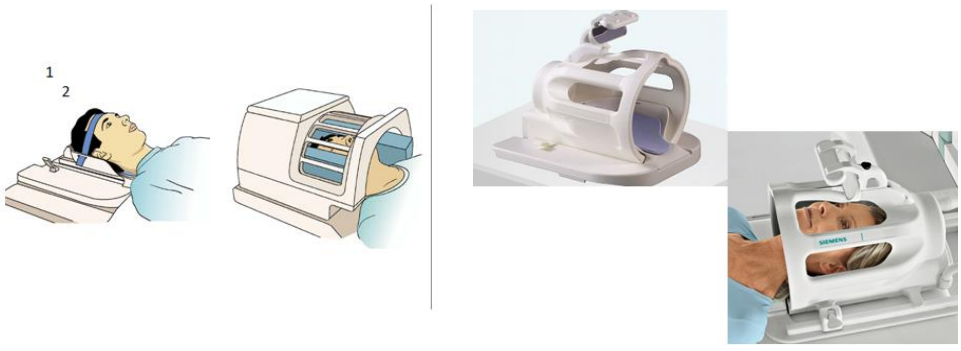

Fig (2.12) Shows the head coil

2-5-5 Protocol for brain imaging:

There are many different combinations of se-quences possible for brain MR imaging. According to Robertson (2011), standard clinical protocol for the brain should contain the following precontrast sequences: T1- and T2-weighted turbo spin echo and Fluid Attenuation Inversion Recovery (FLAIR) sequences in the transversal plane, starting from rostral to the center of the first cervical vertebra (C1). Robertson (2011) and Wessmann (2006) used T2-weighted gradient echo sequence in the transverse plane to find blood degradation products in dogs with hypothetical hemorrhagic infarcts, hemorrhagic meta-stasis, coagulopathies or angiostrongylosis. A T2-weighted sequence in the sagittal plane is helpful in assessing transtentorial and foramen magnum herniation, and cauda fossa morphology. proposed that standard brain imaging protocol should include T2-weighted fast spin echo (FSE) in the transverse and sagittal plane, dorsal FLAIR, transverse T1-weighted gradient echo (GE) or spin echo (SE), and dorsal T1-weighted high-resolution three-dimensional (3D) sequences, both before and after contrast administration.(Konar et al 2011) .

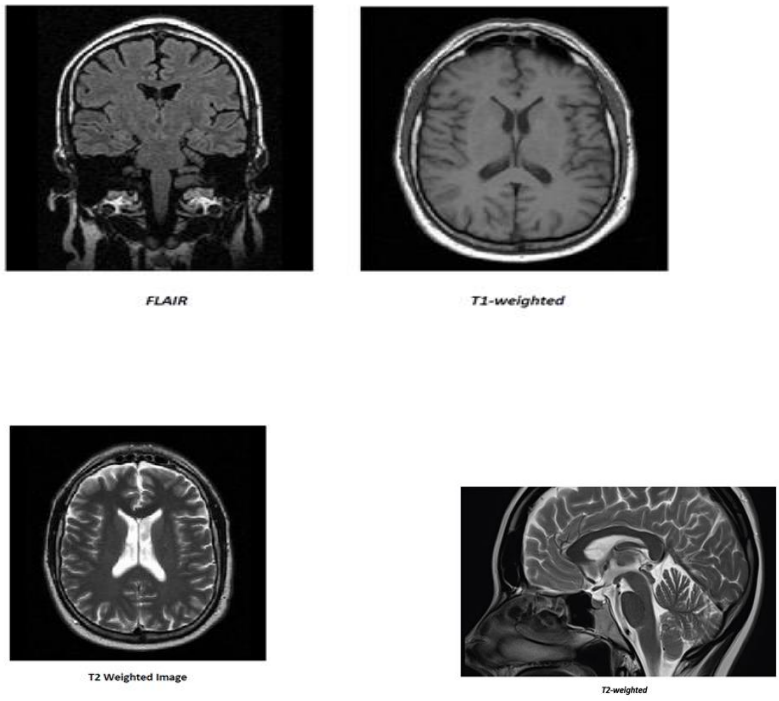

Fig (2.13) shows different sequences of the brain. (Westbrook, 2008).

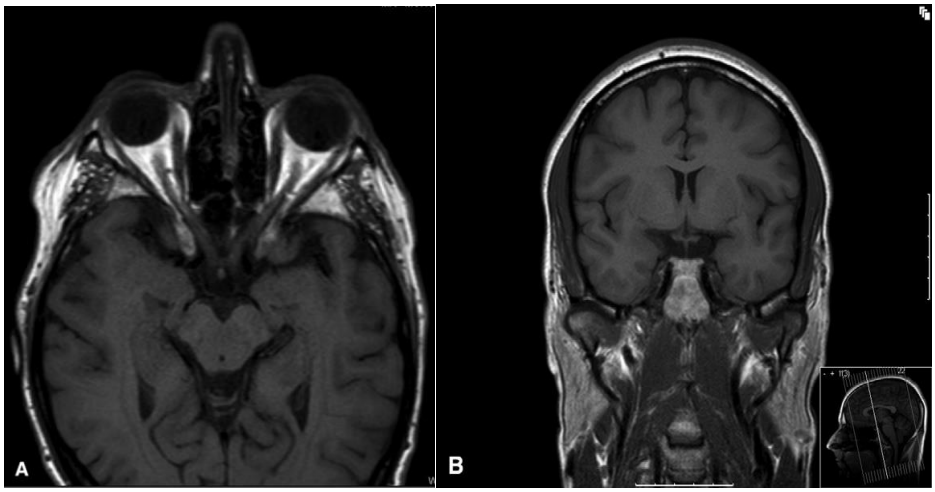

Fig (2-14): T1 weighted axial& coronal MRI showing the position and immediate relationship of the chiasm to adjacent anatomical structures. (Bergland et al., 1968).

2-13 Previous Studies

Holly D.et al in 2016 studied the uses of magnetic resonance imaging to assess visual deficits. Their review aims to investigate structural, chemical and functional effects of eye diseases, using MRI, including: macular degeneration, retinitis pigmentosa, glaucoma, albinism, and amblyopia.

Their Findings showed: Structural MRI has demonstrated significant abnormalities within both grey and white matter densities across both visual and non-visual areas. Functional MRI studies have also provided extensive evidence of functional changes throughout the whole of the visual pathway following visual loss, particularly in amblyopia. MR spectroscopy techniques have also revealed several abnormalities in metabolite concentrations in both glaucoma and age-related macular degeneration.

They concluded that future MRI will likely play an important role in assessing the impact of eye disease on the visual pathway and how it progresses over time.

Krista R et al (2014) studied the Altered anterior visual system development following early monocular enucleation, NeuroImage In Their study; they sought to determine the consequences of early monocular enucleation on the morphological development of the anterior visual pathway including the optic chiasm and lateral geniculate nucleus.

They Concluded that The novel finding of an asymmetry in morphology of the anterior visual system following long-term survival from early monocular enucleation indicates altered postnatal visual development.

Lenhart PD et al (2014) studied The role of magnetic resonance imaging in diagnosing optic nerve hypoplasia Their purpose is To establish objective

lower limits of normal optic nerve (ON) size in children based on high-resolution orbital magnetic resonance imaging (MRI).

Its Case-control study of patients with ON hypoplasia vs normal controls.

A neuroradiologist made 4 measurements of each ON at 2 locations (5 mm posterior to the optic disc and just posterior to the optic canal) in patients with ON hypoplasia and controls aged 0–17 years from an academic eye center and children's hospital. Primary analyses were performed using mixed linear models.

Their Results showed that Measurements were made in 26 cases of clinically confirmed ON hypoplasia and 31 controls ,Concluded that Age was independently associated with normal ON size by MRI and should be taken into consideration when evaluating ON hypoplasia, based on MRI criteria. .

F. Fadzli et al (2013) studied MRI of optic tract lesions: Review and correlation with visual field defects This review considers the chiasmatic and post-chiasmatic causes of visual disturbances, with an emphasis on magnetic resonance imaging (MRI) techniques. Newer MRI sequences are considered, such as diffusion-tensor imaging. MRI images are correlated with perimetric findings in order to demonstrate localization of lesions in the visual pathway. This may serve as a valuable reference tool to clinicians and radiologists in the early diagnostic process of differentiating causes of various visual field defects in daily practice.

Menjot de Champfleura et al (2013) studied the optic chiasm and retrochiasmal visual pathways, Diagnostic and Interventional Imaging

The exploration of the chiasmal and retrochiasmal visual pathways is based on magnetic resonance imaging. The exploration protocol is based on MRI with T1-weighted sagittal sections, then T2- and T1-weighted coronal

Yang QT et al (2011) studied the Evaluation of traumatic optic neuropathy in patients with optic canal fracture using diffusion tensor magnetic resonance imaging Their Objective is to investigate the role of diffusion tensor magnetic resonance imaging (DT-MRI) in the evaluation of traumatic optic neuropathy (TON). Its included Six patients with TON underwent DT-MRI, provides valuable information for evaluating the fibers of optic nerves in TON.

Schmitz B et al (2007) studied the morphology of the optic chiasm in albinism. . This atypical decussation leads to morphological changes of the optic chiasm including a reduced chiasm width with larger angles between optic nerves and tracts which can be shown by magnetic resonance imaging.

Elena Vinogradov et al (2005)studied Magnetic Resonance Imaging of the Optic Chiasm at 3T Their Purpose: To evaluate techniques for anatomical and phys iological imaging of the intracranial optic nerve (ON), optic chiasm (OC), and optic tract (OT) at 3T with the aim of visualizing axonal damage in multiple sclerosis (MS).

They Concluded that by using 3T and a custom- designed, four-channel head coil, it is possible to acquire high- resolution anatomical and physiological images of the OC, ON, and OT. The pilot results presented here pave the way for imaging the anterior visual pathway in patients with MS.

Bernd Schmitz et al (2003) studied configuration of the optic chiasm in humans with albinism as revealed by magnetic resonance imaging, To determine whether the size and configuration of the optic chiasm in humans with albinism is different from that in normal control subjects.

Seventeen patients and 15 control subjects underwent magnetic resonance imaging of the entire head. The most striking difference in the measurements was in the width of the chiasm, which differed significantly between patients (10.3 0.8 mm [SD]) and con- trol subjects (12.9 0.8 mm). it concluded that the albino group showed significantly smaller chiasmatic widths, smaller optic nerves and tracts, and wider angles between nerves and tracts. Statistical morphometry showed a different configuration of the optic chiasm.

R A Rachel, et al (1997) studied Measurement of the Normal Optic Chiasm on Coronal MR Images, their purpose is to develop an objective method for measuring the optic chiasm and to document its normal range in size. their results were the mean area of the optic chiasm was 43.7 mm2, with a standard deviation of 5.21.The mean width was 14.0 mm, with a standard deviation of 1.68.

Parravano et al 1993 studied Dimensions of the optic nerves, chiasm, and tracts: MR quantitative comparison between patients with optic atrophy and normal. their aims assessed The dimensions of the optic nerves, chiasm, and tracts were determined in normal patients and in patients with clinical evidence of optic atrophy to establish whether there was a significant difference between the two groups.

The normal mean dimensions were (height x width): optic tracts 2.8 x 5.1 mm; nerves 3.0 x 5.9 mm; chiasm 3.5 x 15.0 mm. The mean dimensions in

the optic atrophy group were significantly less ($p < 0.01$): optic tract 2.1 x 4.7 mm; nerve 2.7 x 5.8 mm; chiasm 2.6 x 12.6 mm.

Daniels et al(1984) studied Magnetic resonance imaging of the optic nerves and chiasm which was compared with computed tomography (CT) in 4 healthy volunteers, 4 patients without orbital or chiasmal abnormalities, and 4 patients with tumor (anterior clinoid meningioma in 2, optic nerve glioma in 1, and optic nerve sheath meningioma in 1).

MR was found to be effective in demonstrating the optic nerves and related structures, particularly the intracanalicular portion of the nerve which is difficult to see with CT. Best results were achieved with partial saturation recovery (SR) images; inversion recovery (IR) and spin echo (SE) techniques were less successful because of decreased spatial resolution (in the case of SE) as well as difficulty in seeing the anterior clinoid processes. As axial views cannot always distinguish the ethmoid sinus tissue from the optic nerve, it may be necessary to employ both axial and coronal images.

CHAPTER THREE

Materials and Methods

3.1 Material:

This study was done at Khartoum state hospitals, Royal care hospital & Antalya medical center in Khartoum Sudan, during the period from November2015to July 2018. All the patients underwent MRI brain. . Data was collected with help of a Performa including name, gender, age, symptoms, and findings of the brain MRI

3.1.1: The Sample.

This retrospective and prospective study included 205 Sudanese patients, 43.4 %(89) were female, 56.6 %(116) were male. With different ages ranges (between 16-78 years old) attending radiology department. 172 patients were diagnosis by experienced radiologists as a normal MRI brain, 33 patients having pathological changes such as: astrocytoma, brain atrophy mastoiditis, metastasis brain, optic atrophy, and sinusitis. 30 of them had visual impairments, 38 of them had headache, and 45 of them had optic atrophy.

3.1.2: Equipment used

Toshiba Excel art Vantage 1.5 T & General electric 1.5 T: The Toshiba Excel art Vantage 1.5T MRI machine is an ultra-short, ultra-wide-bore system with adjustable lighting and ventilation features designed to ease patient anxiety without sacrificing performance. Powered by Atlas, the Toshiba Excel art Vantage 1.5T MRI system delivers high-resolution images across the entire body with faster imaging times.

The GE Signa 1.5 T MRI system is the most compact MR imaging system offered by GE, taking up 30%less site space than comparable systems.

Equipped with detachable gantry table that will improve workflow as well as patient safety.

3.2 **Method**:

3.2.1: Study protocols (Techniques)

MRI studies were performed whole body MR systems using standard imaging head coil. Routine brain MRI was performed in 3 orthogonal planes, The patient lies supine on the examination couch. examined general brain. Used head coil, (these are placed over-head but should not touch the patient). The patients are positioned so that the longitudinal alignment light lies in the midline , and the horizontal alignment light passes through the nasion Straps and foam pads are used for immobilization. T1,T2,FLAIR.DW weighted imaging was performed in the axial, coronal & sagittal plane. all images were 5mm in thick with a0.5 mm space between slices.in our study we used coronal T2 only for measurements

The data were collected from the PAC'S system on the selected hospitals; the cases were transferred to a workstation, at which the width & height of the optic chiasm were measured on the coronal section, using region interest (ROI).

3.2.2 Methods of measurements:

For purposes of standardization of positioning, the coronal section passing through the optic chiasm 3mm anterior to the pituitary fossa was used for all measurements of the optic chiasm. The width of the optic chiasm was measured horizontally at the centering point; chiasm the height of the optic chiasm was measured in the midline and was taken in mm. The data gathered were presented in tables and figure when appropriate. The mean and range was used to evaluate statistically the results. The means were calculated using the excel software & SPSS program.

3.2.3: Statistical analysis

All data obtained in the study were documented and analyzed using SPSS program version 21.Continuous data are presented as mean ± standard deviation (SD) and compared using the *t* test. Categorical data were expressed as percent frequencies, and differences between proportions were compared. Statistical correlation between continuous variables was tested using the Pearson's product-moment coefficient of correlation (r). All tests of significance were two tailed and a p-value < 0.05 was considered statistically significant. All analyses were performed using SPSS version 21. statistical software.

3.2.4: Ethical issues:

Approval for this study was obtained from RCIH & Antalya medical center

Verbal consent was taken from the participants.

There is no identification or individual patient detail was published.

Chapter Four

Results

4.1 Results:

Table (4.1): Shows distribution of study sample according to gender (n205):-

Gender		Frequency	Percent
	Female	89	43.4
	Male	116	56.6
	Total	205	100.0

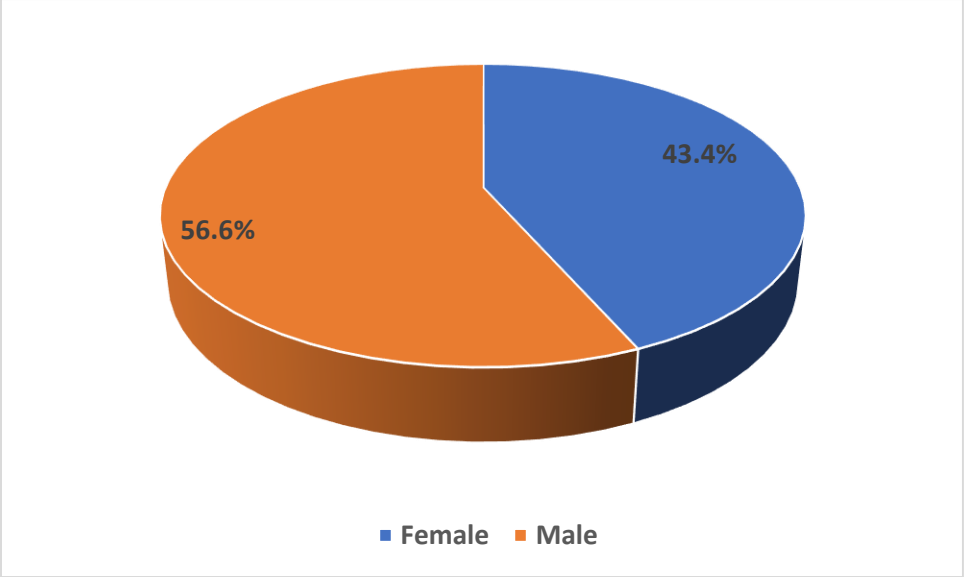

Fig (4.1): shows distribution of study sample according to gender (n205)

Table (4.2): Mean, median, standard deviation, minimum and maximum of study participants age (n=205)

Statistics		
Age /years		
N	Valid	205
	Missing	0
Mean		38.94
Median		34.00
Std. Deviation		16.751
Minimum		16
Maximum		78

Table (4.3): shows distribution of study sample according to age group (n=205)

Age group / years		**Frequency**	**Percent**
	Less than 20 years old	13	6.3
	20 up to 29 years old	73	35.6
	30 up to 39 years old	42	20.5
	40 up to 49 years old	21	10.2
	50 up to 59 years old	22	10.7
	60 years or more	34	16.6
	Total	205	100.0

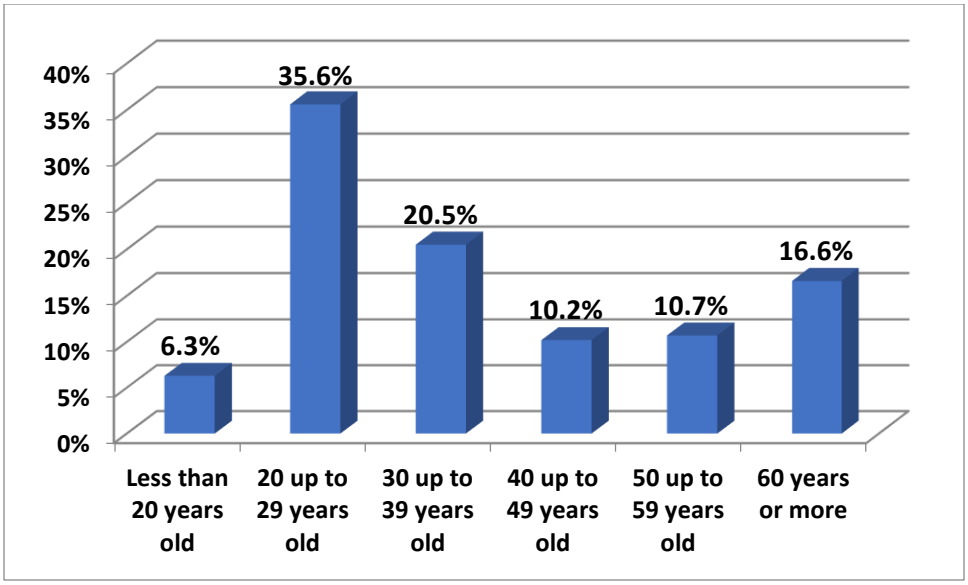

Fig (4.2): shows distribution of study sample according to age group (n=205)

Table (4.4) Shows distribution of study sample according to visual disturbance (n=205)

Visual disturbance		**Frequency**	**Percent**
	No	175	85.4
	Yes	30	14.6
	Total	205	100.0

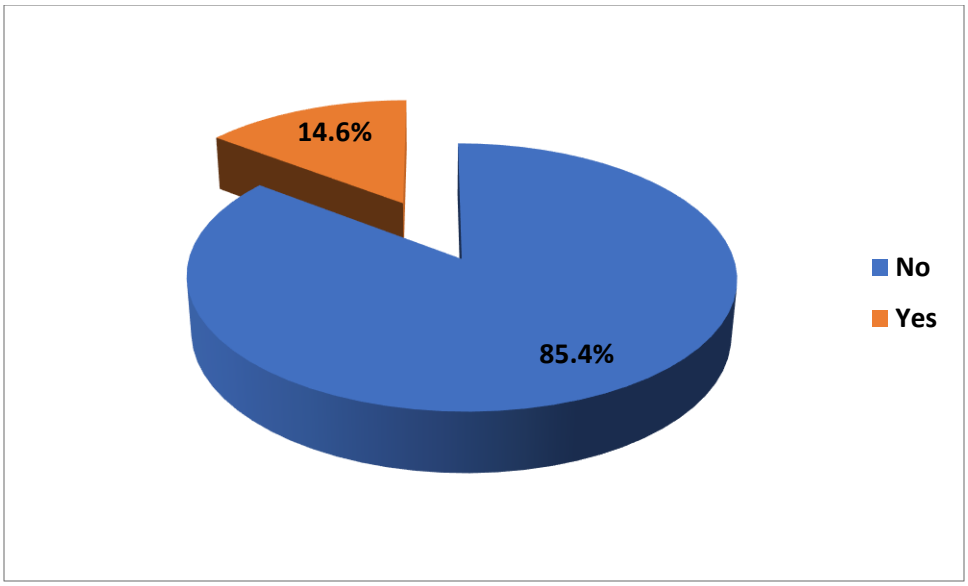

Fig (4.3) Shows distribution of study sample according to visual disturbance (n=205)

Table (4.5): Shows distribution of study sample according to headache (n=205)

Headache	Frequency	Percent
No	167	81.5
Yes	38	18.5
Total	205	100.0

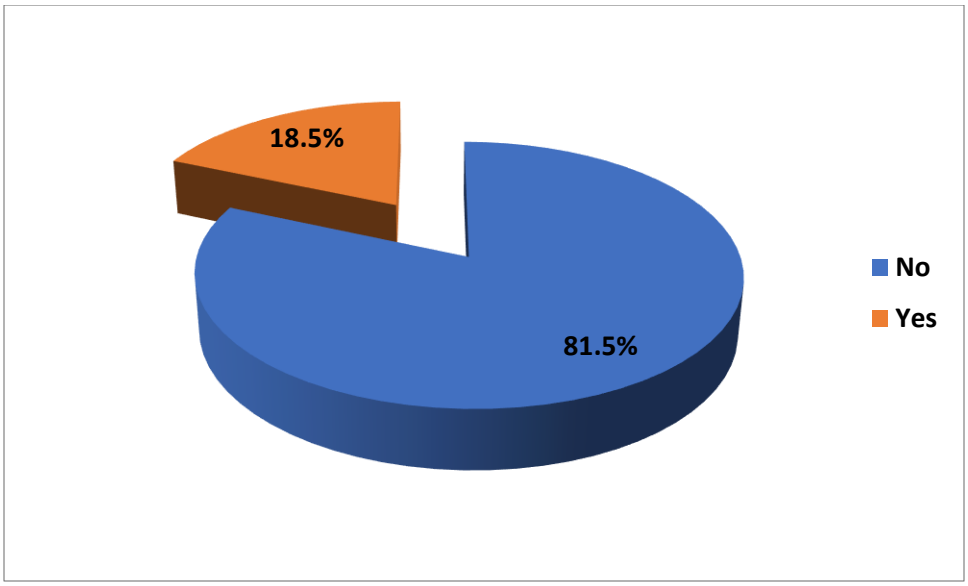

Fig (4.4) Shows distribution of study sample according to headache (n=205)

Table (4.6) Shows distribution of study sample according to optic atrophy (n=205)

Optic atrophy	Frequency	Percent
No	160	78.0
Yes	45	22.0
Total	205	100.0

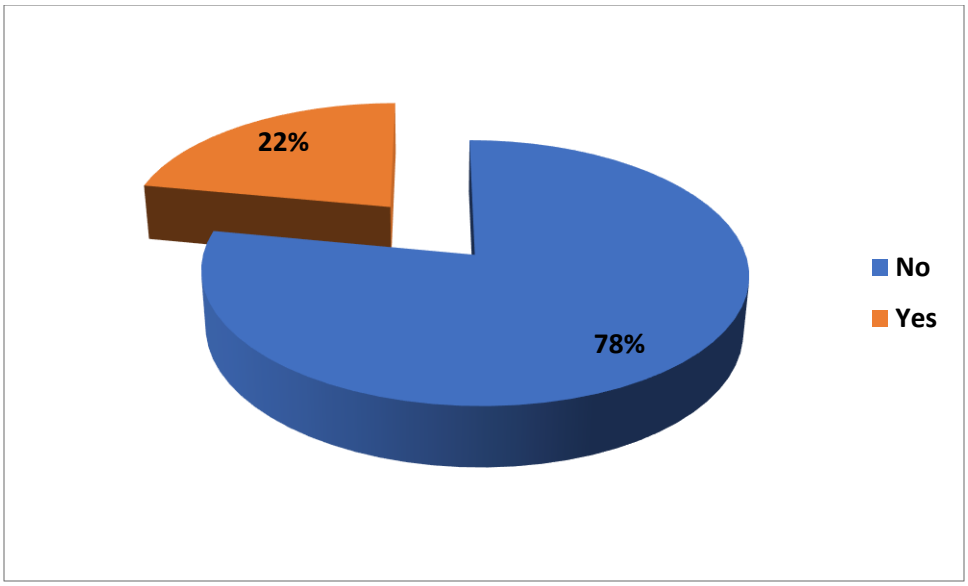

Fig (4.5) Shows distribution of study sample according to optic atrophy (n=205)

Table (4.7) shows mean, median, standard deviation, minimum and maximum of study participants OC width (n=205)

Statistics		
OC width		
N	Valid	205
	Missing	0
Mean		13.0876
Median		13.1100
Std. Deviation		1.22383
Minimum		10.18
Maximum		15.12

Table (4.8): Shows distribution of study sample according to OC width (n=205)

OC width	Frequency	Percent
Less than 12	48	23.4
12 up to 15	152	74.1
More than 15	5	2.4
Total	205	100.0

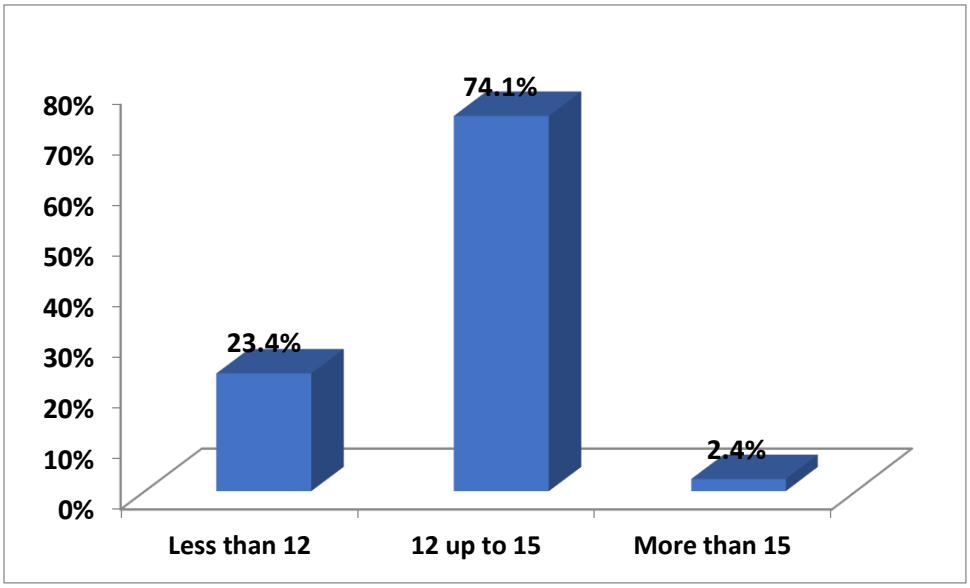

Fig (4.6): Shows distribution of study sample according to OC width (n=205)

Table (4.9): Shows mean, median, standard deviation, minimum and maximum of study participants OC height (n=205)

Statistics		
OC height		
N	Valid	205
	Missing	0
Mean		2.4733
Median		2.4500
Std. Deviation		.15472
Minimum		2.11
Maximum		3.04

Table (4.10) Shows distribution of study sample according to finding (n=205)

	Finding	**Frequency**	**Percent**
	Astrocytoma	1	.5
	Brain atrophy	3	1.5
	Mastoiditis	13	6.3
	metastasis brain	1	.5
	Normal brain	172	83.9
	Optic atrophy	1	.5
	Sinusitis	13	6.3
	Sinusitis/ Mastoiditis	1	.5
	Total	205	100.0

Table (4.11): shows the relationship between finding with OC width and OC height: (n=205)

Report			
Finding		OC width	OC height
Astrocytoma	N	1	1
	Mean	14.4900	2.5500
	Std. Deviation	.	.
Brain atrophy	N	3	3
	Mean	13.6567	2.4300
	Std. Deviation	.00000	.00000
Mastoiditis	N	13	13
	Mean	13.3177	2.5377
	Std. Deviation	1.24897	.21009
metastasis brain	N	1	1
	Mean	11.5800	2.4600
	Std. Deviation	.	.
Normal brain	N	172	172
	Mean	13.0429	2.4619
	Std. Deviation	1.21003	.14613
Optic atrophy	N	1	1
	Mean	11.1600	2.4600
	Std. Deviation	.	.
Sinusitis	N	13	13
	Mean	13.4269	2.5592
	Std. Deviation	1.40862	.20217
Sinusitis/mastoid ties	N	1	1
	Mean	13.7000	2.5500
	Std. Deviation	.	.
Total	N	205	205
	Mean	13.0876	2.4733
	Std. Deviation	1.22383	.15472

Table (4.12): Shows cross tabulation between gender and finding: (n=205)

Finding * Gender Cross tabulation					
			Gender		Total
			Female	Male	
Finding	**Astrocytoma**	Count	1	0	1
		%within Finding	100.0%	0.0%	100.0%
	Brain atrophy	Count	2	1	3
		%within Finding	66.7%	33.3%	100.0%
	Mastoiditis	Count	6	7	13
		%within Finding	46.2%	53.8%	100.0%
	metastasis brain	Count	1	0	1
		%within Finding	100.0%	0.0%	100.0%
	Normal brain	Count	72	100	172
		%within Finding	41.9%	58.1%	100.0%
	Optic atrophy	Count	1	0	1
		%within Finding	100.0%	0.0%	100.0%
	Sinusitis	Count	6	7	13
		%within Finding	46.2%	53.8%	100.0%
	Sinusitis/mastoiditis	Count	0	1	1
		%within Finding	0.0%	100.0%	100.0%
Total		Count	89	116	205
		%within Finding	43.4%	56.6%	100.0%

Table (4.13): Shows cross tabulation between finding and visual disturbance: (n =205)

Crosstab					
			Visual disturbance		**Total**
			No	Yes	
Finding	**Astrocytoma**	Count	1	0	1
		% within Finding	100.0%	0.0%	100.0 %
	Brain atrophy	Count	2	1	3
		% within Finding	66.7%	33.3%	100.0 %
	Mastoiditis	Count	9	4	13
		% within Finding	69.2%	30.8%	100.0 %
	metastasis brain	Count	0	1	1
		% within Finding	0.0%	100.0%	100.0 %
	Normal brain	Count	157	15	172
		%within Finding	91.3%	8.7%	100.0 %
	Optic atrophy	Count	0	1	1
		%within Finding	0.0%	100.0%	100.0 %
	Sinusitis	Count	6	7	13
		%within Finding	46.2%	53.8%	100.0 %
	Sinusitis/ mastoidites	Count	0	1	1
		%within Finding	0.0%	100.0%	100.0 %
Total		Count	175	30	205
		%within Finding	85.4%	14.6%	100.0 %

Table (4.14): shows cross tabulation between finding headache: (n=205)-

Crosstab					
			Headache		Total
			No	Yes	
Finding	**Astrocytoma**	Count	0	1	1
		% within Finding	0.0%	100.0%	100.0%
	Brain atrophy	Count	2	1	3
		% within Finding	66.7%	33.3%	100.0%
	Mastoiditis	Count	2	11	13
		% within Finding	15.4%	84.6%	100.0%
	metastasis brain	Count	1	0	1
		% within Finding	100.0%	0.0%	100.0%
	Normal brain	Count	151	21	172
		% within Finding	87.8%	12.2%	100.0%
	Optic atrophy	Count	1	0	1
		% within Finding	100.0%	0.0%	100.0%
	Sinusitis	Count	9	4	13
		% within Finding	69.2%	30.8%	100.0%
	Sinusitis/mastoiditis	Count	1	0	1
		% within Finding	100.0%	0.0%	100.0%
Total		Count	167	38	205
		% within Finding	81.5%	18.5%	100.0%

Table (4, 15): shows the relationship between age group with OC width and OC height: - (n=205)

Age group / years		OC width	OC height
Less than 20 years old	N	13	13
	Mean	13.8246	2.4654
	Std. Deviation	1.03548	.11333
20 up to 29 years old	N	73	73
	Mean	13.2103	2.4840
	Std. Deviation	1.22627	.15020
30 up to 3 years old	N	42	42
	Mean	13.0100	2.4598
	Std. Deviation	1.31356	.17637
40 up to 49 years old	N	21	21
	Mean	13.0519	2.4924
	Std. Deviation	1.40503	.18485
50 up to 59 years old	N	22	22
	Mean	13.0264	2.4723
	Std. Deviation	.97444	.14973
60 years or more	N	34	34
	Mean	12.7000	2.4588
	Std. Deviation	1.10934	.13967
Total	N	205	205
	Mean	13.0876	2.4733
	Std. Deviation	1.22383	.15472

Table (4.16): shows the relationship between gender with OC width and OC height: - (n=205)

Gender		OC width	OC height
Female	N	89	89
	Mean	13.0652	2.4872
	Std. Deviation	1.24378	.15503
Male	N	116	116
	Mean	13.1048	2.4626
	Std. Deviation	1.21343	.15430
Total	N	205	205
	Mean	13.0876	2.4733
	Std. Deviation	1.22383	.15472

Table (4.17) shows of study normal sample of OC width (n=172)

Statistics		OC width
N	Valid	172
	Missing	0
Mean		13.0429
Median		13.0050
Std. Deviation		1.21003
Range		4.94
Minimum		10.18
Maximum		15.12

Table (4.18) shows of study normal sample of OC height (n= 172)

Statistics	OC height
N	172
Mean	2.4619
Median	2.4450
Std. Deviation	.14613
Range	.86
Minimum	2.18
Maximum	3.04

Table (4.19) shows of study abnormal sample of OC width (n=33)

		OC width
N	Valid	33
	Missing	0
Mean		13.3206
Median		13.6900
Std. Deviation		1.28733
Range		3.98
Minimum		11.11
Maximum		15.09

Table (4.20) shows of study abnormal sample of OC height (n=33)

		OC height
N	Valid	33
	Missing	0
Mean		2.5324
Median		2.4700
Std. Deviation		.18490
Range		.78
Minimum		2.11
Maximum		2.89

Chapter five

5.0 Discussion, Conclusion and Recommendation

5-1 Discussion

The optic chiasm is an important landmark when interpreting magnetic resonance (MR) examinations of the brain. MR imaging has proved to be the method of choice for examining the optic chiasm, especially coronal high-field T1, T2, and PD-weighted imaging, which seems to depict the anatomy to the best advantage**.** A small chiasm can be an indication of several disorders, the most common of which is septooptic dysplasia, and a large chiasm can be the result of glioma, meningioma, lymphoma, or hemorrhage. The diagnosis of atrophy or enlargement of the chiasm has largely been made by interpretation, and is therefore highly subjective and variable among observers. We retrospectively reviewed 205 coronal MR images of the normal and abnormal brain and measured the width and height of the optic chiasm to determine a range of normal values. These references can potentially aid in the early detection of infiltrating processes of the chiasm and can be used in cases in which the diagnosis of optic chiasm atrophy is uncertain.

In our study. We used a 5.0-mm isotropic voxel size, we think that use of the section on which the chiasm is largest will minimize error, Presumably, thinner sections would increase edge sharpness and decrease measuring error even more, but they would be impractical from a time-management standpoint as well as for decreasing the signal-to-noise ratio. The used of 5mm slice thickness in the study .affected partial volume, which was make the range of chiasm look wider. whereas in two previous studies considered by paraveno et al (1993) &wenger F et al (1997) are used 3.0-mm thick coronal slices.

The coronal slices measured by Wagner et al (1993) are oriented perpendicular to the normal optic chiasm, which the optic chiasm width varies (10.5–18.5 mm [vs]. 10.18–15.09 mm in our study). .while Parravano et al (1993). showed the normal range width between 10.6 mm and 17.4 mm (2 SD from the mean) This smaller range may reflect the smaller sample size. Chiasms outside these ranges should be considered abnormal and prompt further investigation. , at the abnormal group ,the mean width of optic chiasm was 13.32 ± 1.28 standard deviation while the mean height of the optic chiasm was 2.53 ± 0.184 standard deviation. The coronal slices measured by Bernd Schmitzr et al (2003). is oriented perpendicular to the optic chiasm, which the mean chiasmatic width of alpinism group were 12.9 ± 0.8 mm ·while Parravano et al (1993). showed The mean dimensions in the optic atrophy group were chiasm width 2.6 and height 12.6 mm. Paravano et al(1993), they used hand held digital calipers for the measurements .while we used the computer offer (ROI) to more accurate measurements. the measurements were made on T2 weighted MRI, while Andrew L et al (1997) believed that the most accurate measurements were made on T1wheigted images as the chiasm was seen best at this sequences

Breakdown by age and gender showed an expected no significant in the measurement of the chiasm as patients got older, This were consider different from what mentioned by Paraveno et al (1993)&Wenger F et al (1997) which they showed a decrease in width with increasing age. correlation with gender yielded no significant difference, the same as we found in our study.

Our intention was to measure the optic chiasm on a presumed standard T2-weighted coronal MR image, The calculated measurement of the normal optic chiasm on MR sections can be used as a comparative standard by

which to detect relatively smaller or larger chiasms, regardless of whether the measurements are in exact ratio to the actual nerve. For the above-mentioned the number of adult patients in this study was relatively low compared to previous studies in this age group, while the NO of subjects were slightly high. The three-dimensional shape of the chiasm makes it a difficult organ to measure. We believe that the accurate measurements can be made on T2-weighted MR images, as the chiasm is seen clearly on this sequence in our opinion. Use of a selected image from a coronal MR study of the chiasm allows this structure to be seen and measured without having to determine reproducible anterior and posterior cut-off points, which would be necessary on axial images. Although there may be some variation due to differences in sections among studies, we think that use of the section on which the chiasm is largest will minimize error. Not all studies are suitable for this calculation, such as those with enough motion or noise to make the margins of the chiasm indistinct. However, in a lot of our patients, the images had enough detail to make reproducible determination of the borders possible, and no special imaging of the Sella was necessary. The statistical analysis show not significant difference between finding and OC width (p value 0.30) &OC height (p value0.265)these results were illustrated in table (4.11),and these finding were due to the sample size of abnormal subjects, which were 33 cases (Brain atrophy ,mastoiditis and sinusitis were affected visual disturbance) with P value significant 0.01on cross tabulation between finding and visual disturbance in Table(4.14) also they were affected headache) with P value significant 0.01on cross tabulation between finding headache table (4.15).

5-2 Conclusion

This study concluded that the Sudanese population morphology is slightly different from other populations mentioned in the previous studies Mean of total optic chiasm width was 13.08 ± 1.22 standard deviation, height was 2.47 ± 0.154 standard deviation

In .the normal cases the optic chiasm width ranged from 10.18 mm to 15.12 mm ,the optic chiasm height range from 2.18mm to 3.04 mm, in the abnormal cases the optic chiasm width ranged from 11.11 mm to 15.09 mm ,the optic chiasm height range from 2.11mm to 2.89 mm Coronal MRI may prove beneficial for demonstration of optic chiasm anatomy .The width and height of the optic chiasm can be measured with the use of commercially available software, which allows an objective estimate of the chiasm's size. Knowledge of the normal size range of the optic chiasm can be helpful in the early detection of some disorders

Our study suggests that optic chiasms with a width on coronal MR images between 10.18 mm and 15.12 mm (1.2 SD from the mean) and a height between 2.11 mm and 3.04 mm (.15 SD from the mean) can be considered definitely normal. Chiasms outside these ranges should be considered abnormal and prompt further investigation.

Knowledge of the normal size range of the optic chiasm can be helpful in the early detection of some disorders

These measurements can be calculated with any of the multitude of commercial software currently available, and most MR units now in use have the capabilities to furnish the ROI measurements

The calculated measurement of the normal optic chiasm on MR sections can be used as a comparative standard by which to detect relatively smaller or larger chiasms, regardless of whether the measurements are in exact ratio to the actual nerve

5-3 Recommendations:

- More research on this field must be done and coordinated with ophthalmologist and radiologists.
- More precise measurements may be possible using dedicated multi–plane high resolution MRI images from larger sample size of abnormal volunteers.
- Learning more about the disease which may affect the chiasm area.
- Add additional protocol on brain MRI sequences with thin slice cuts to make the measurements more accurate.

REFERENCES

Akhadder A, El Hassani MY, Chakir N, Jiddane M. 2001. Optochiasmatic tuberculoma: complication of tuberculous meningitis. Report of a case and review of the literature. J Neuroradiol 28:137–142.

Barber AN, Ronstrom GN, Muelling RJ Jr. 1954. Development of the visual pathway: optic chiasm. Arch Ophthalmol 52:447–453.

Beck RW, Schatz NJ, Savino PJ. 1983. Involvement of the optic chiasm, optic tract and geniculo- calcarine visual system in multiple sclerosis. Bull Soc Belge Ophtalmol 208:159–191.

Bensing S, Hulting AL, Hoog A, Ericson K, Kampe O. 2007. Lymphocytic hypophysitis: report of two biopsy- proven cases and one suspected case with pituitary auto- antibodies. J Endocrinol Invest30:153–162.

Bergland RM, Ray BS, Torack RM. 1968. Anatomical variations in the pituitary gland and adjacent structures in 225 human autopsy cases. J Neurosurg 28:93–99.

Bernd Schmitz, Torsten Schaefer, Christoph M. Krick, Wolfgang Reith, Martin Backens,and Barbara Käsmann-Kellner، 2003 Configuration of the Optic Chiasm in Humans with Albinism as Revealed by Magnetic Resonance Imaging, Jan;44(1):16-21.

Brazis PW, Miller NR. Miller NR, Newman NJ, 2005. Walsh and Hoyt's Viruses (except retroviruses) and viral diseases. IN: Clinical Neuro ophthalmology. 6th Ed. Philadelphia: Lippincott Williams and Wilkins. p 3115–3284.

Brodsky MC, Hoyt WF, Barnwell SL, Wilson CB. 1988. Intrachiasmatic craniopharyngioma: a rare cause of chiasmal thickening. J Neurosurg 68:300–302.

Cappelli C, Grill J, Raquin M, Pierre- Kahn A, Lellouch- Tubiana A, Terrier- Lacombe MJ, Habrand JL, Couanet D, Brauner R, Rodriguez D, Hartmann O, Kalifa C. 1998. Long term follow up of 69 patients treated for optic pathway tumours before the chemotherapy era. Arch Dis Child 79:334–338.

Chang GY, Keane JR. 2001. Visual loss in Cysticercosis: analysis of 23 patients. Neurology 57:545–548.

Cockerham KP, Kennerdell JS, Maroon JC, Bejjani GK. 2005. Tumors of the meninges and related tissues: meningiomas and sarcomas. . Walsh and Hoyt's Clinical Neuro- ophthalmology. 6th Ed. Philadelphia: Lippincott Williams and Wilkins. p 1486–1518.

Cohen DB, Glasgow BJ. 1993. Bilateral optic nerve Cryptococcus in sudden blindness in patients with acquired immune deficiency syndrome. Ophthalmology 100:1689–1694.

Crocker M, Desouzza R, King A, Connor S, Thomas N. 2008. Cavernous haemangioma of the optic chiasm: a surgical review. Skull Base 18:201–212.

Cushing H, Walker CB. 1915. Distortions of the visual fields in cases of brain tumor. Brain 37:341–400.

Dalan R, Leow MK. 2008. Pituitary abscess: our experience with a case and a review of the literature. Pituitary 11:299–306.

Daniels DL, Herfkins R, Gager WE, Meyer GA, Koehler PR, Williams AL, Haughton VM., 1984 Magnetic resonance imaging of the optic nerves and chiasm. Radiology. Jul;152(1):79-83.

De Bellis A, Ruocco G, Battaglia M, Conte M, Coronella C, Tirelli G, Bellastella A, Pane E, Sinisi AA, Bizzaro A, Bellastella G. 2008. Immunological and clinical aspects of lymphocytic hypophysitis. Clin Sci (Lond) 114:413–421.

Domingues FS, Marcondes de Souza J, Chagas H, Cimelli L, Vaisman M. 2002. Pituitary tuberculoma: an unusual lesion of sellar region. Pituitary 5:149–153.

Dutton JJ. 1992. Optic nerve sheath meningiomas. Surv Ophthalmol 37:167–183.

Dutton JJ. 1994. Gliomas of the anterior visual pathway. Surv Ophthalmol 38:427–452.

Frohman LP, Frieman BJ, Wolansky L. 2001. Reversible blindness resulting from optic chiasmitis secondary to systemic lupus erythematosis. J Neuroophthamol 21:18–21.

Frohman LP, Guirgis M, Turbin RE, Bielory L. 2003. Sarcoidosis of the anterior visual pathway: 24 new cases. J Neuroophthalmol 23:190–197.

Greven CM, Singh T, Stanton CA, Martin TJ. 2001. Optic chiasm, optic nerve, and retinal involvement secondary to varicella- zoster virus. Arch Ophthalmol 119:608–610.

Guoth MS, Kim J, de Lotbiniere AC, Brines ML. 1998. Neurosarcoidosis presenting as hypopituitarism and a cystic pituitary mass. Am J Med 315:220–224.

Hamilton AM, Garner A, Tripathi RC, Sanders MD. 1973. Malignant optic nerve glioma: report of a case with electron microscopic study. Br J Ophthalmol 57:253–264.

Hassan A, Crompton JL, Sandhu A. 2002. Traumatic chiasmal syndrome: a series of 19 patients. Clin Exp Ophthalmol 30:272–280.

Herrera, Eloisa & García Frigola, Cristina. (2008). Genetics and development of the optic chiasm. Frontiers in bioscience : a journal and virtual library. 13. 1646-53. 10.2741/2788.

Horton JC. 1997. Wilbrand's knee of the primate optic chiasm is an artefact of monocular enucleation. Trans Am Ophthalmol Soc 95:579–609.

Hoyt WF, Fletcher WA, Imes RC. 1987. Chiasmal gliomas: appearances and long term changes demonstrated by computerized tomography. Prog Exp Tumor Res 30:113–121.

Hoyt WF, Luis O. 1969. The primate chiasm: details of the visual fiber organisation studied by silver impregnation techniques. Clin Neurosurg 17:189–208.

Humphrey PRD, Moseley IF, Ross Russell RW. 1982. Visual field defects in obstructive hydrocephalus. J Neurol Neurosurg Psychiatry 45:591–597.

Kawasaki A, Purvin VA. 2009. Idiopathic chiasmal neuritis: clinical features and prognosis. Arch Ophthalmol 127:76–81.

Kennard and R.J. Leigh,. 2011 All rights reserved Handbook of Clinical Neurology, Editors Elsevier B.V Vol. 102 (3rd series) Neuro-ophthalmology

Kidd D, Beynon HLC. 2003. Neurological complications of systemic sarcoidosis (Review). Sarcoidosis Vasc Diff Lung Dis 20:85–94.

Kidd D, Wilson PL, Unwin B, Dorward N. 2003. Lymphocytic hypophysitis presenting in the first trimester of pregnancy. J Neurol 250:1385–1387

Kidd DP, Revesz T, Miller NR. 2006. Neurological complications of Rosai- Dorfman syndrome. Neurology 67:1551–1555.

Kidd, D. (2011) The optic chiasm. Handb Clin Neurol.;102:185-203.

Koszman JJ, Rouleau J, Gaunt M, Kardon RH, Wall M, Lee AG. 2008. Neuro- ophthalmic Sarcoidosis: the University of Iowa experience. Semin Ophthalmol 23:157–168.

Krista R. Kelly, LarissaMcKettonb, Keith A. Schneider, Brenda L. Gallie, Jennifer K.E. Steeves , (2014) Altered anterior visual system development following early monocular enucleation, NeuroImage: Clinical 4 72–81

Kupfer C, Chumbley L, Downer J de C. 1967. Quantitative histology of the optic nerve, optic tract and lateral geniculate nucleus of man. J Anat 101:393–401.

Larmonde A, Larmonde P. 1977. L'atteinte de genou posterieur du chiasma. Rev Otoneuroophtalmol 49:1–2.

Leigh RJ, Zee DS. 1991. Diagnosis of central disorders of ocular motility. In: The Neurology of Eye Movements. 2nd Ed. Philadelphia : FA Davis Co. p 392–393.

Lenhart PD, Desai NK, Bruce BB, Hutchinson AK, Lambert SR 2014 ,The role of magnetic resonance imaging in diagnosing optic nerve hypoplasia. Am J Ophthalmol. ;158(6):1164-1171.

Meissirel C, Chalupa LM. 1994. Organisation of pioneer retinal axons within the optic tract of the Rhesus monkey. Proc Nat Acad Sci USA 91:906–910.

Miller NR. 2008. Primary and secondary tumors of the optic nerve and its sheath. . Philadelphia: Butterworth- Heinemann. p 215–223.

Mtanda AT, Cruysberg JRM, Merx JL, Thyssen HOM. 1986. The ocular presentation of intracranial epidermoid tumours: a review of 37 cases from the literature. Neuroophthalmology 6:223–230.

Murphy M, Timms C, McKelvie P, Dowling A, Trost N. 2003. Malignant optic nerve glioma: metastasis to the spinal neuroaxis. J Neurosurg 98:110.

Newman NJ, Lessell S, Wintertorn JMS. 1991. Optic chiasmal neuritis. Neurology 41:1203–1210.

O'Connell JEA. 1973. The anatomy of the optic chiasma and heteronymous hemianopia. Journal of Neurology, Neurosurgery, and Psychiatry.;36(5):710-723.

Osher RH, Corbett JJ, Schatz NJ, Savino PJ, Orr LS. 1978. Neuro-ophthalmological complications of enlargement of the third ventricle. Br J Ophthalmol 62:536–542.

Parravano JG, Toledo A, Kucharczyk W., 1993 Dimensions of the optic nerves, chiasm, and tracts: MR quantitative comparison between patients with optic atrophy and normals., J Comput Assist Tomogr. Sep-Oct;17(5):688-90.

Purvin V, Herr GJ, De Myer W. 1988. Chiasmal neuritis as a complication of Epstein- Barr virus infection. Arch Neurol 45:458–460.

R A Rachel, B E Reese, 1997 Optic Nerve, Optic Chiasm, and Optic Tracts Andrew L. Wagner, F. Reed Murtagh, Ken S. Hazlett, and John A. Arrington Measurement of the Normal Optic Chiasm on Coronal MR Images, AJNR: 18, April

Rao VJ, James RA, Mitra D. 2008. Imaging characteristics of common suprasellar lesions with emphasis on MRI findings. Clin Radiol 63:939–947.

Rudd A, Rees JE, Kennedy P, Weller RO, Blackwood W. 1985. Malignant optic nerve gliomas in adults. J Clin Neuro- Ophthalmol 5:238–243.

Sami DA, Saunders D, Thompson DA, Russell- Eggitt IM, Nischal KK, Jeffrey G, Dattani M, Clement RA, Liasis A, Taylor DS. 2005. The achiasmia syndrome: congenitally reduced chiasmal decussation. Br J Ophthalmol 89:1311–1317.

Sato N, Sze G, Endo K. 1998. Hypophysitis: endocrinologic and dynamic MR findings. AJNR 19:439–444.

Schaeffer JP. 1924. Some points on the regional anatomy of the optic pathway, with special reference to tumors of the hypophysis cerebri; and resulting ocular changes. Anat Res 28:243–279.

Schlechte JA. 2003. Prolactinoma. N Engl J Med 349:2035–2041.

Seror R, Mahr A, Ramanoelina J, Pagnoux C, Cohen P, Guillevin L. 2006. Central nervous system involvement in Wegener granulomatosis. Medicine (Baltimore) 85:54–65.

Sibony PA, Lessell S, Wray S. 1982. Chiasmal syndrome caused by arteriovenous malformations. Arch Ophthalmol 100:438–442.

Silverman IE, Liu GT, Bilaniuk LT, Volpe NJ, Galetta SL. 1995. Tuberculous meningitis with blindness and perichiasmal involvement on MRI. Pediatr Neurol 12:65–67.

Stippler M, Gardner PA, Snyderman CH, Carrau RL, Prevedello DM, Kassam AB. 2009. Endoscopic endonasal approach for clival chordomas. Neurosurgery 64:268–277.

Tageuchi J, Handa H, Nasgata I. 1978. Suprasellar germinoma. J Neurosurg 49:41–48.

Traquair HM. 1949. An Introduction to Clinical Perimetry. 6th Ed. London: Kimpton.

Unsold R, Hoyt WF. 1980. Band atrophy of the optic nerve. Arch Ophthalmol 98:1637–1638.

Vates GE, Berger MS, Wilson CB. 2001. Diagnosis and management of pituitary abscess: a review of 24 cases. J Neurosurg 95:233–241.

Voelker JL, Campbell RL, Muller J. 1991. Clinical, radiographic and pathological features of symptomatic Rathke's cleft cysts. J Neurosurg 74:535–544.

Wilson CB. 1992. Endocrine- inactive pituitary adenomas. Clin Neurosurg 38:10–31.

Wollschlaeger PB, Wollschlaeger G, Ide CH, Hart WM. 1971. Arterial blood supply of the human optic chiasm and surrounding structures. Ann Ophthalmol 3:862–864.

Yang QT, Fan YP, Zou Y, Kang Z, Hu B, Liu X, Zhang GH, Li Y.

Yung TY, Li JYZ, Amato L, Mahadevan K, Phillips PJ, Coates PS, Coates PT. 2008. Pituitary involvement in Wegener's granulomatosis. Pituitary 11:77–84.

Zimmerman LE, Arkfeld DL, Schenken JB, Arkfeld DF, Maris PJ. 1983. A rare choristoma of the optic nerve and chiasm. Arch Ophthalmol 101:766–770.

Appendices:

Appendix A: data collection sheet:

Sudan University of Science and Technology

College of Graduate Studies

PhD of Science in diagnostic

Radiological Technology

The data collection information

Name of Hospitals:

- Antalya medical center
- Royal Care Hospital.

No.	Gender	age	Visual disturbance	symptoms Headache	Optic atroph	OC width	OC height	FINDING
1	M	19	Yes	Yes	Yes	13.76	2.8	sinusitis
2	M	16	yes	Yes	Yes	14.45	2.46	Normal brain
3	M	18	yes	Yes	Yes	13.86	2.46	Mastoiditis
26	**F**	**52**	**yes**	**Yes**	**No**	12.55	2.45	**Normal brain**
28	**F**	**38**	**yes**	**Yes**	**No**	14.35	2.45	**Normal brain**
29	**F**	**43**	**yes**	**Yes**	**No**	14.66	2.46	**Normal brain**
30	**F**	**39**	**yes**	**Yes**	**No**	14.33	2.44	**Normal brain**
31	**F**	**35**	**No**	**No**	**No**	12.55	2.48	**Normal brain**

Appendix B cases:

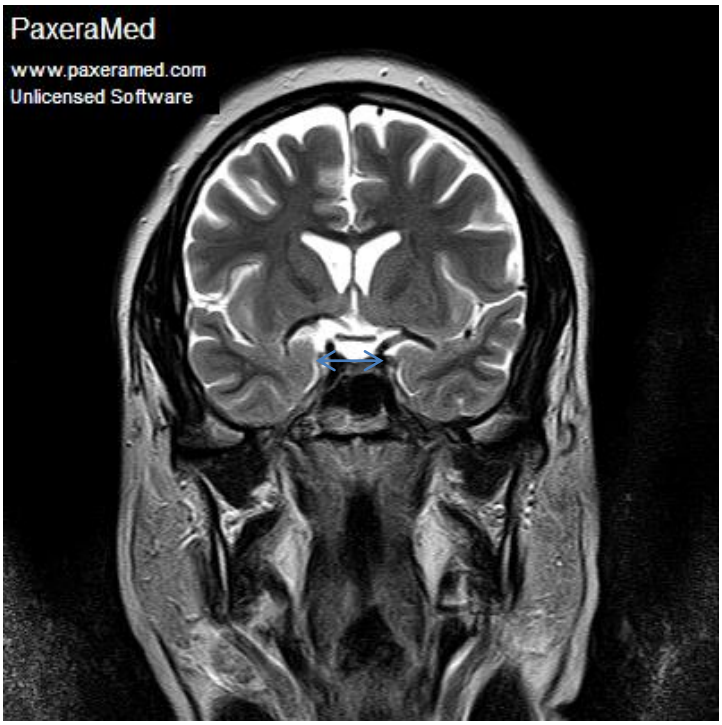

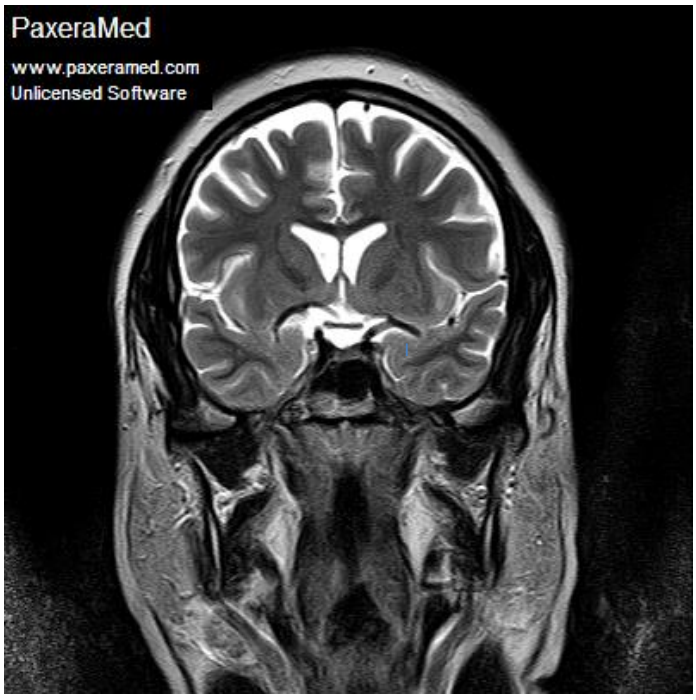

Case(1) coronal T2, Male /age:35 years / optic chiasm width :13.7mm/optic chiasm height: 2.55mm/ finding :sinusitis& mastoiditis

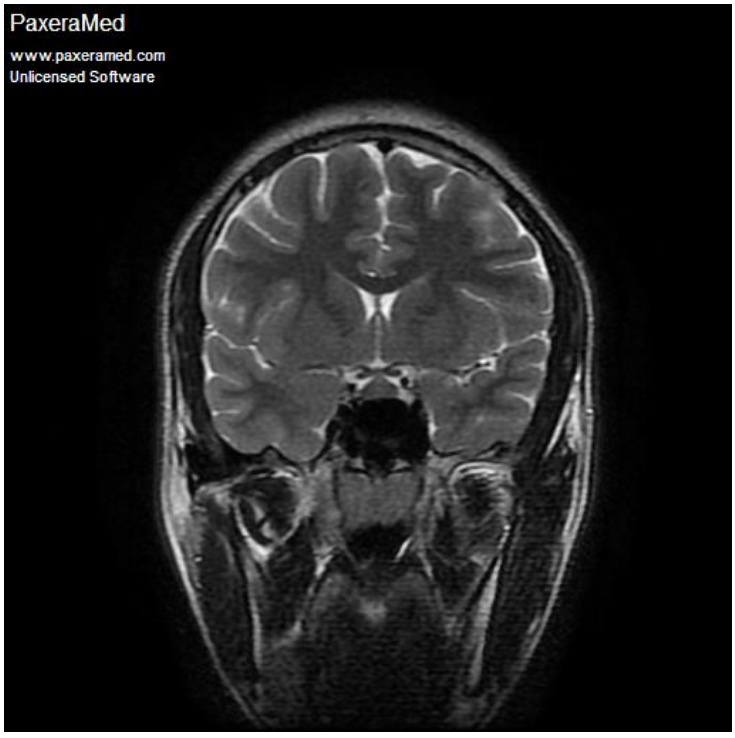

Case(2) coronal T2 Male/age:19 years/optic chiasm width: 13.76mm/optic chiasm height: 2.80mm/ finding: sinusitis

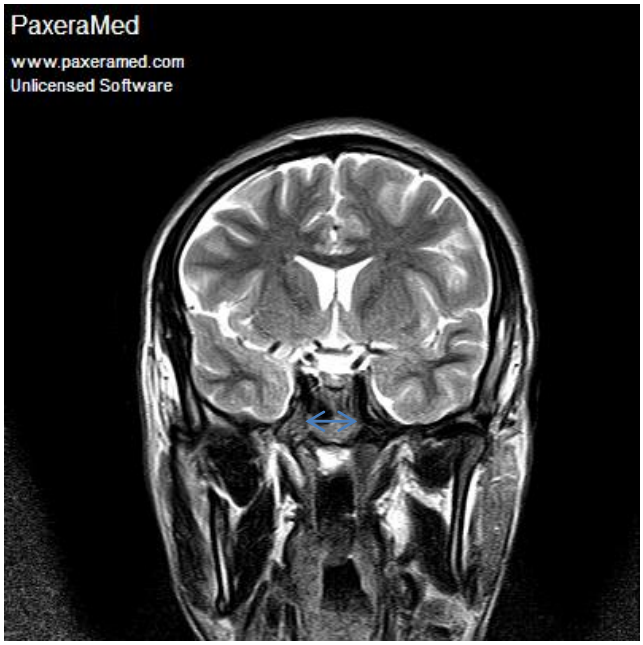

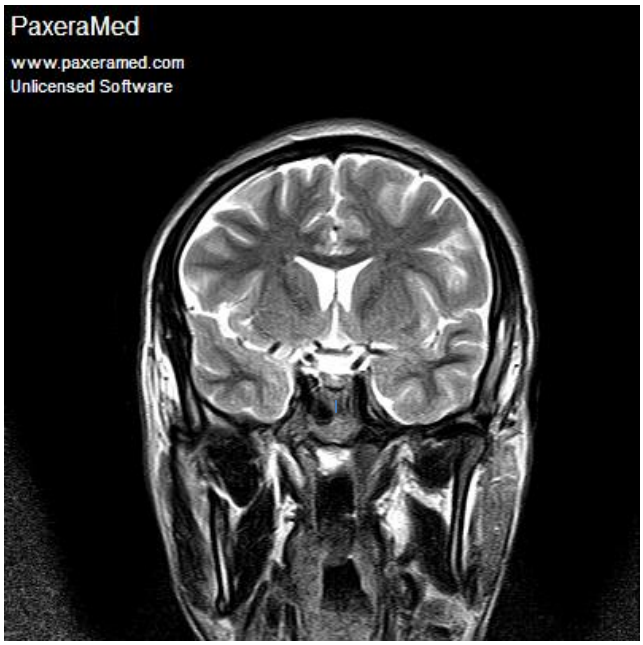

Case(3) coronal T2,male/age:25 years/optic chiasm width: 14.39mm/optic chiasm height: 2.55mm/ finding normal

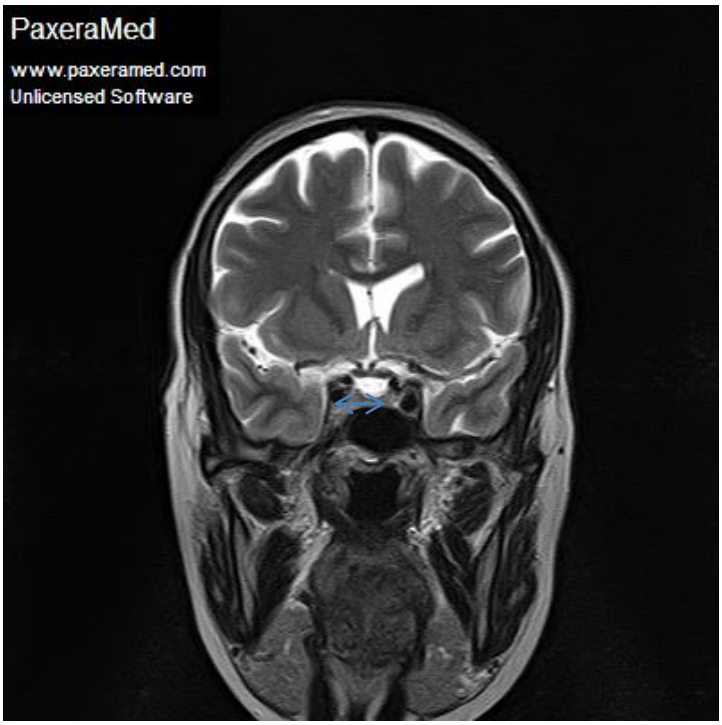

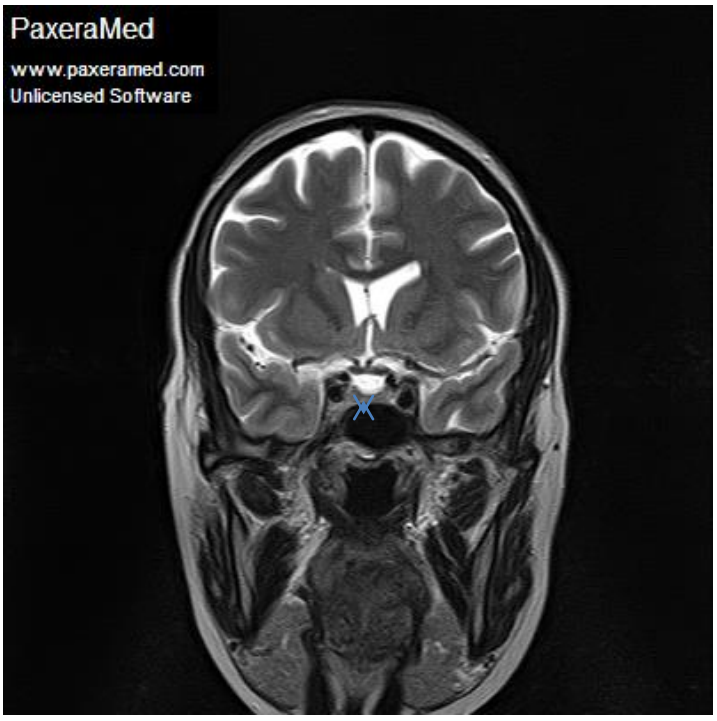

Case(4) coronal T2, male/age:49 years/optic chiasm width14.40 mm/optic chiasm height: 2.46mm/finding :mild sinusitis

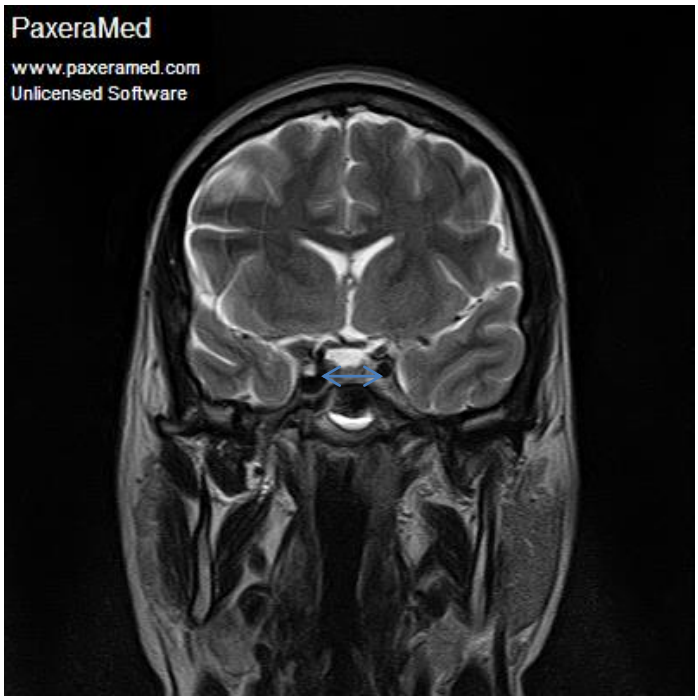

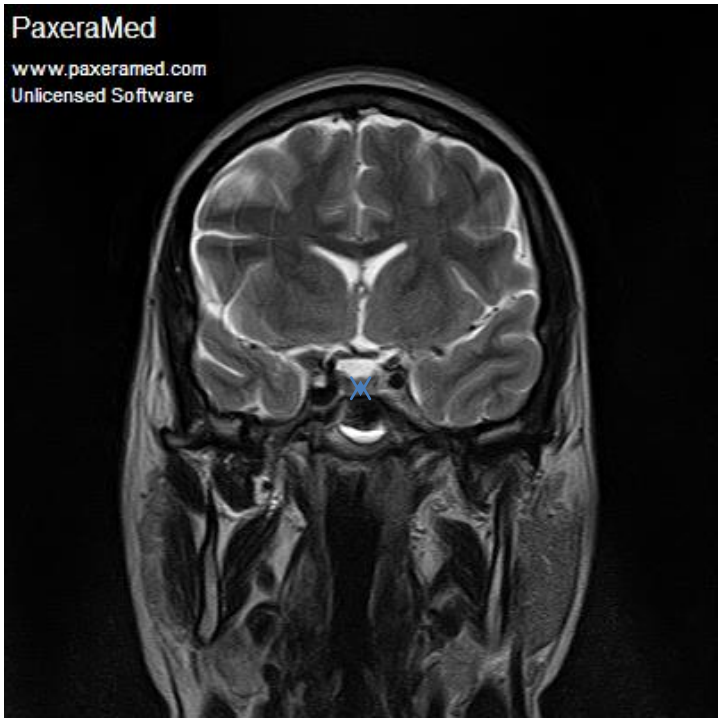

Case(5) coronal T2male/age:26 years/optic chiasm width: 14.04mm/optic chiasm height: 2.55mm/finding: normal

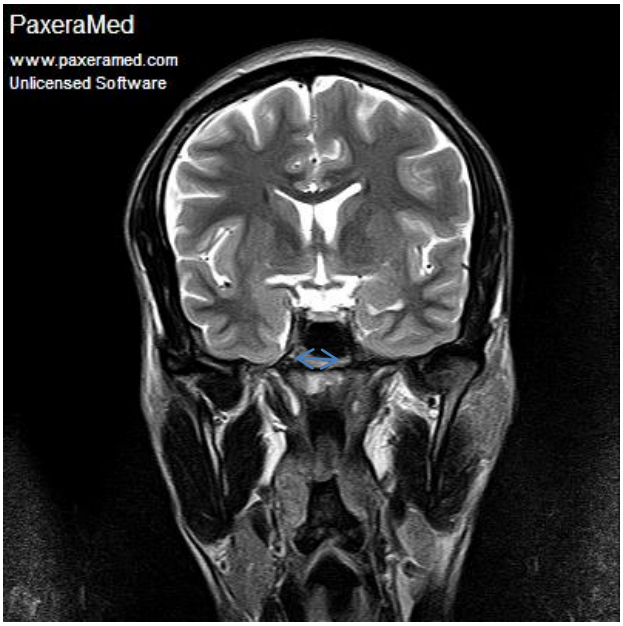

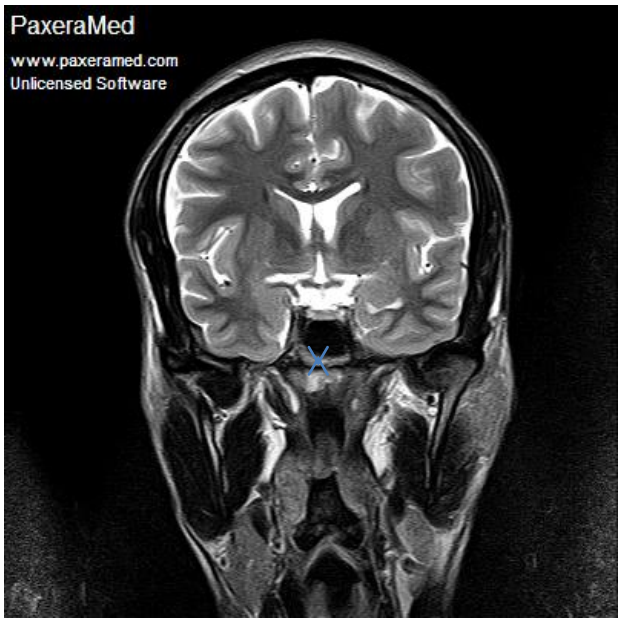

Case(6) coronal T2male/age:32years/optic chiasm width :15.09/optic chiasm height: 2.89mm/finding :normal

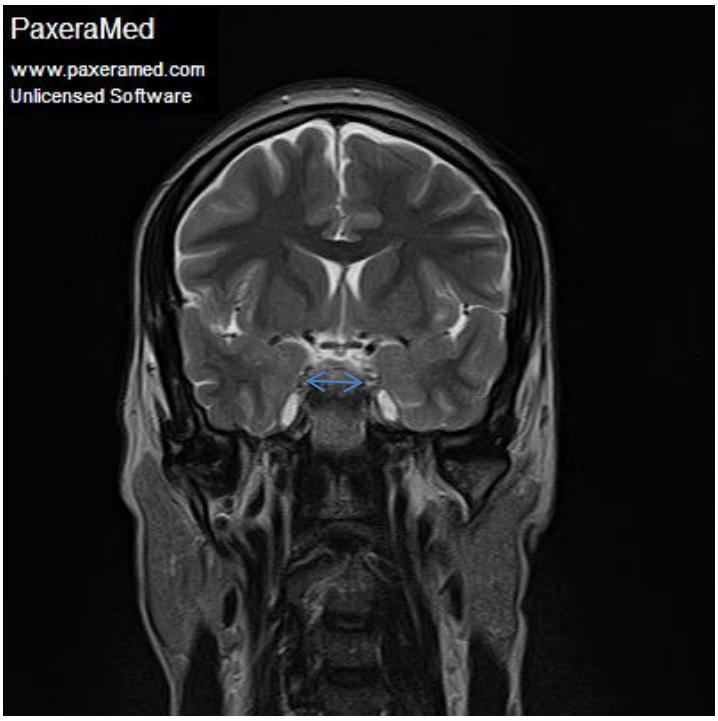

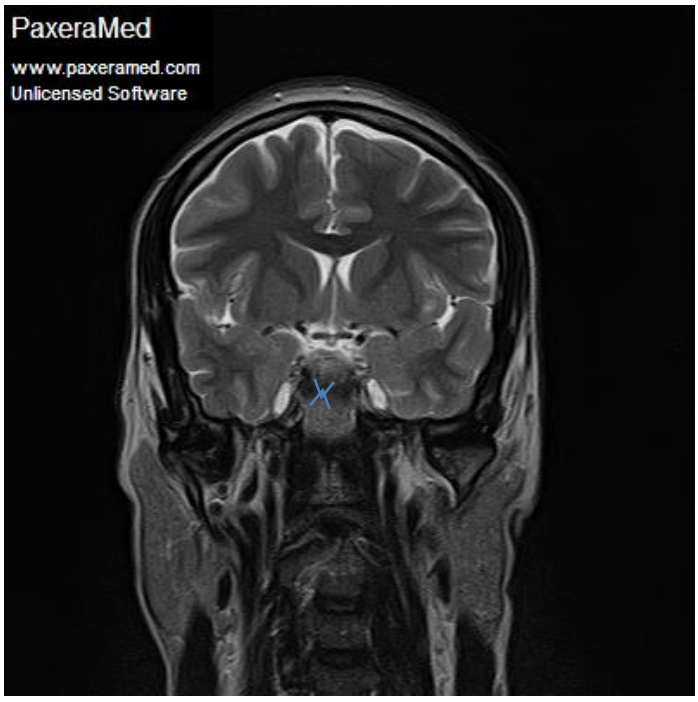

Case(7) coronal T2,male/age:29 years/optic chiasm width: 12.98mm/optic chiasm height: 2.08mm/finding: normal

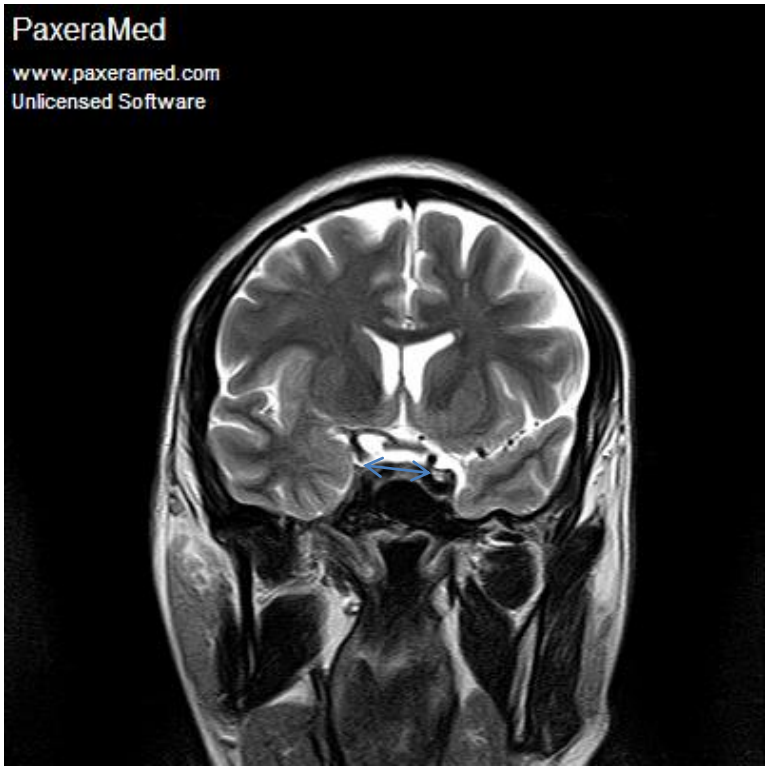

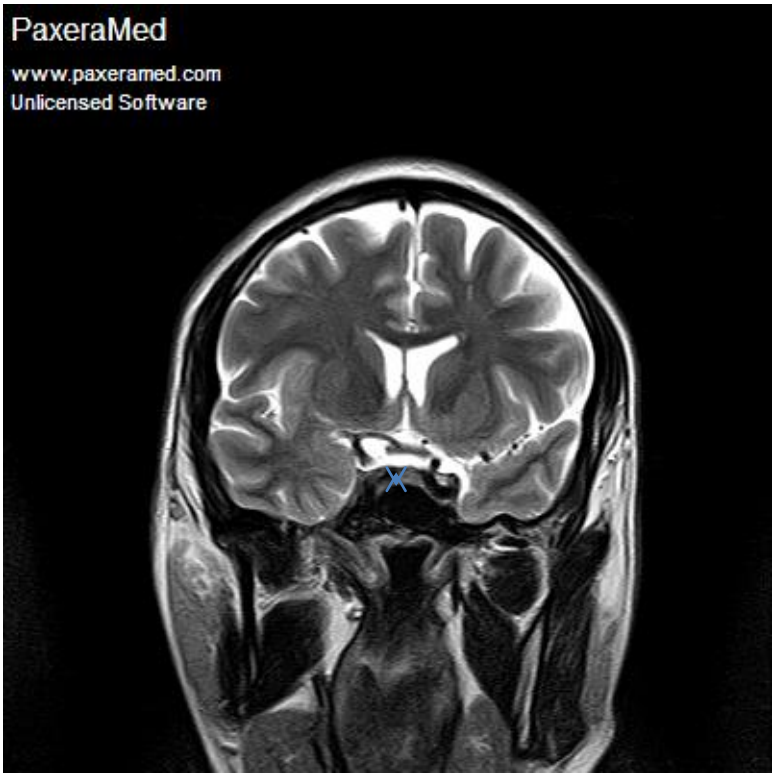

Case(8) coronal T2,male/age:36years/optic chiasm width:13.00 mm/optic chiasm height:2.48mm/finding: normal

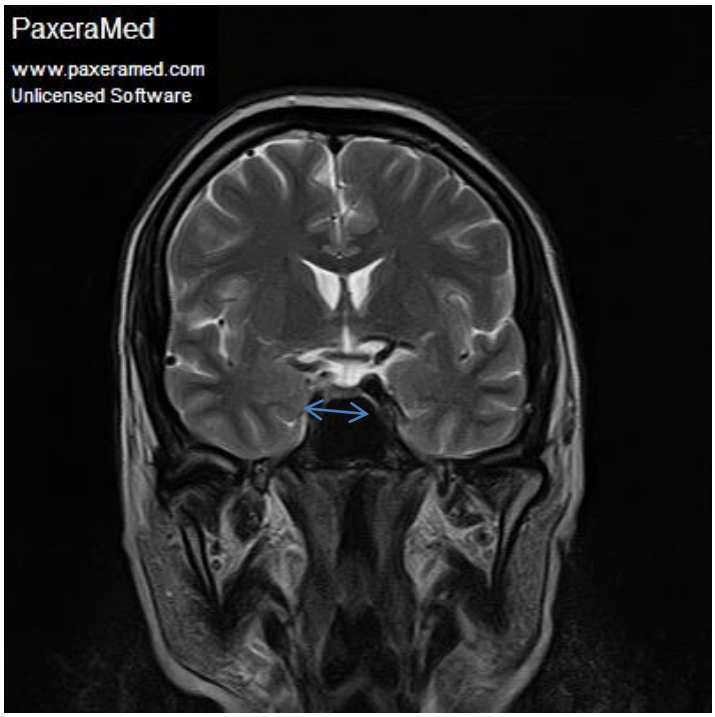

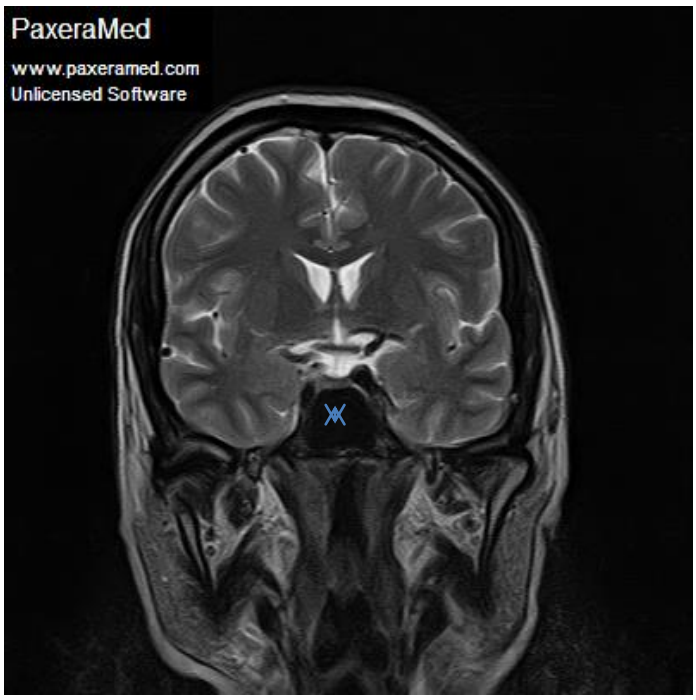

Case(9) coronal T2,male/age:29years/optic chiasm width: 14.42mm/optic chiasm height:2.81mm/finding: normal

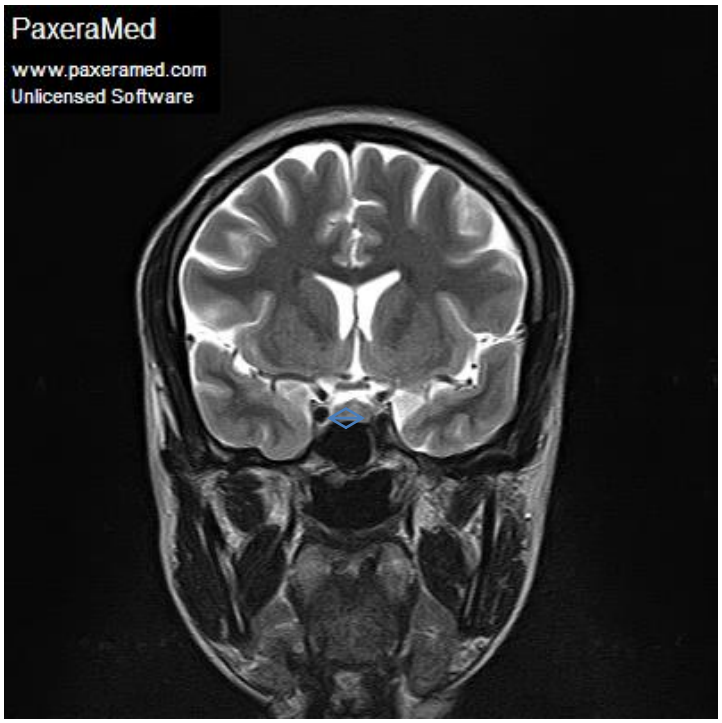

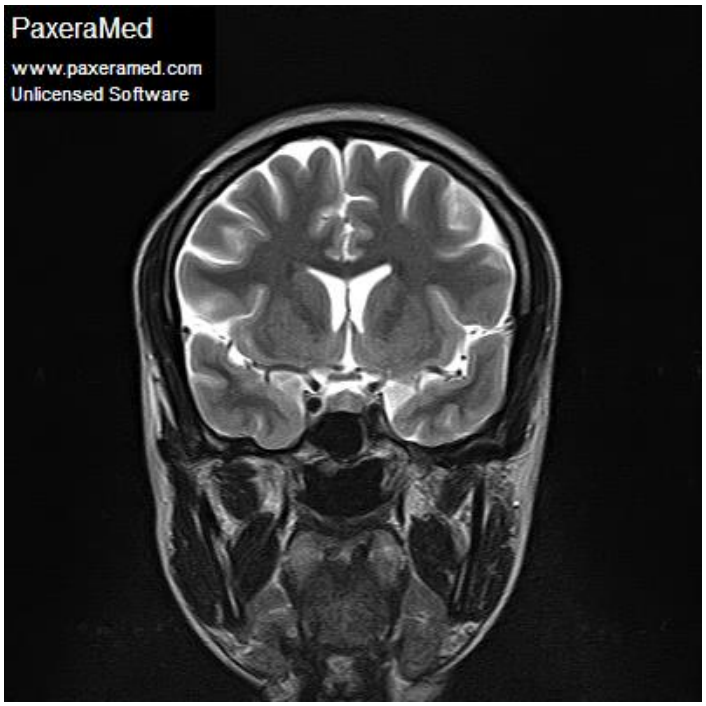

Case(10) coronal T2,female/age:35years/optic chiasm width :11.09mm/optic chiasm height:2.81mm /finding: normal

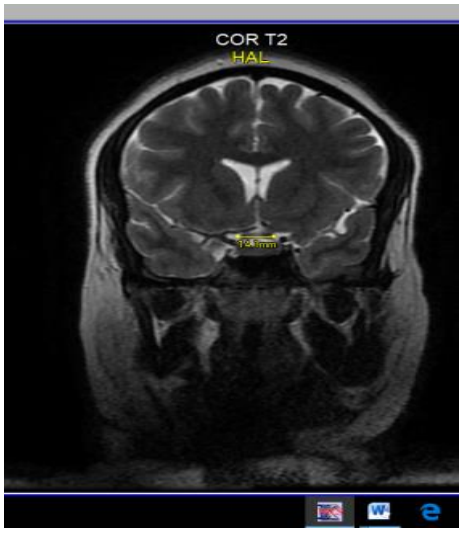

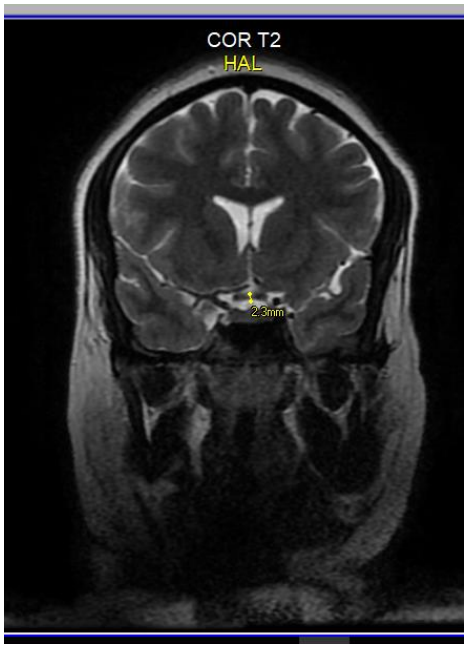

Case(11) coronal T2,female/age:28 years/optic chiasm width: 14.01mm/optic chiasm height:2.3m/finding: normal

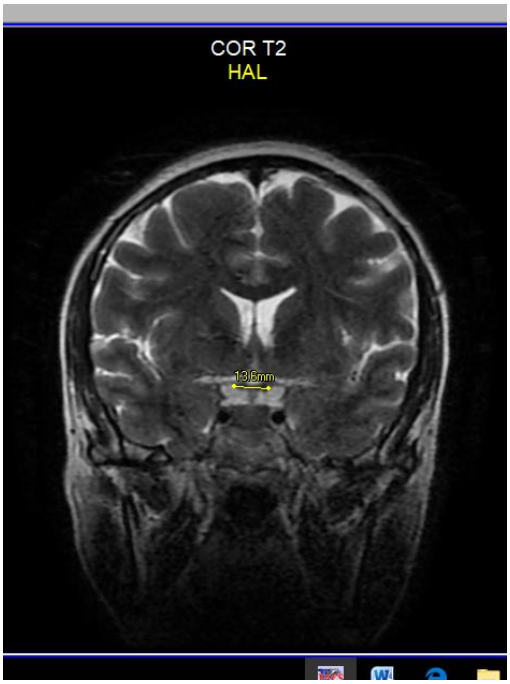

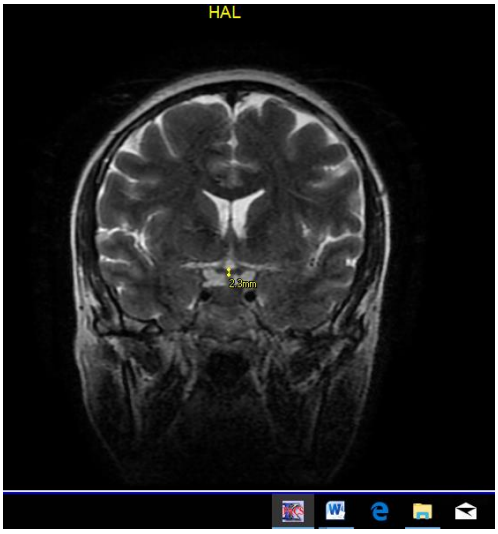

Case(12). coronal T2,female/age:32 years/optic chiasm width: 11.3mm/optic chiasm height: 2.3mm/finding: normal

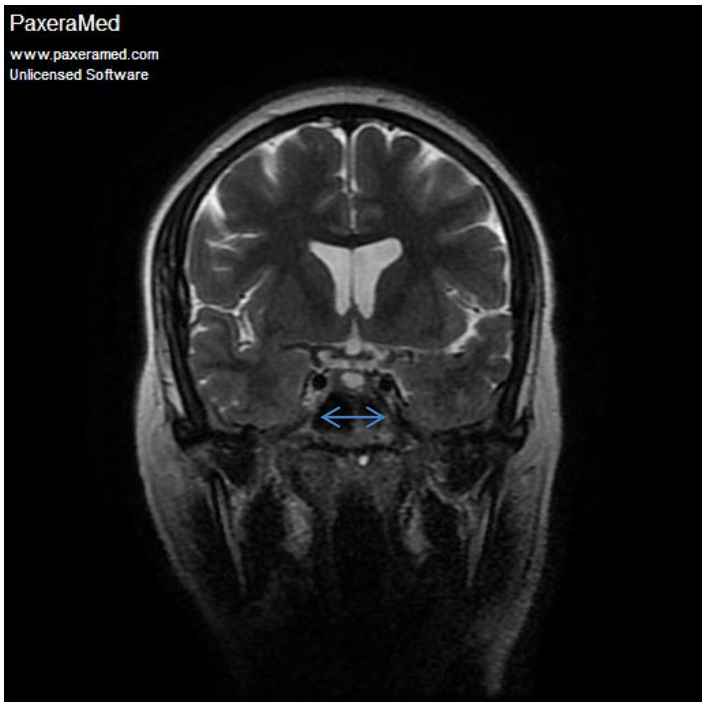

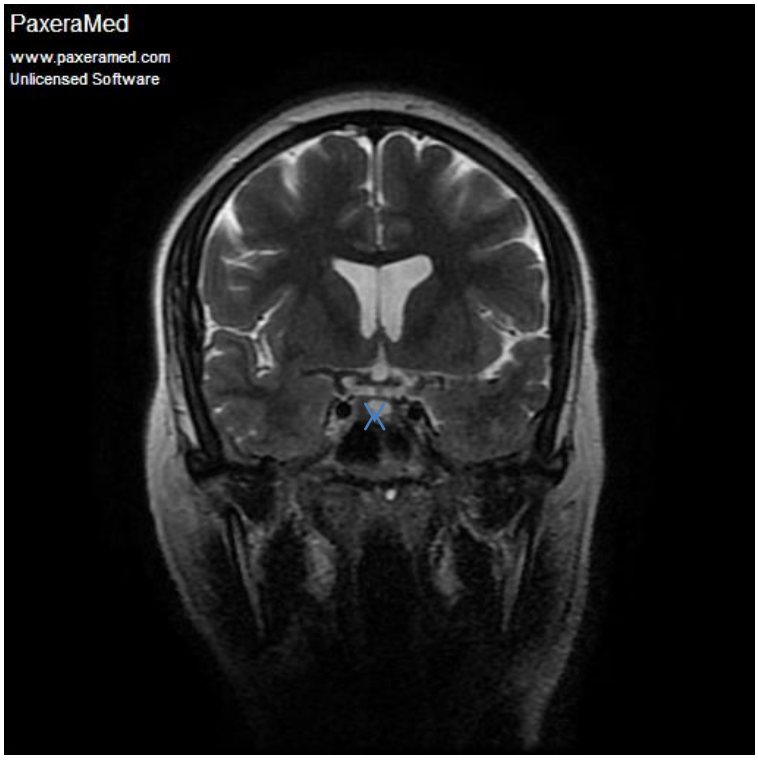

Case(13) coronal T2,female/age:41years/optic chiasm width: 13.64mm/optic chiasm height :2.80mm/finding: normal

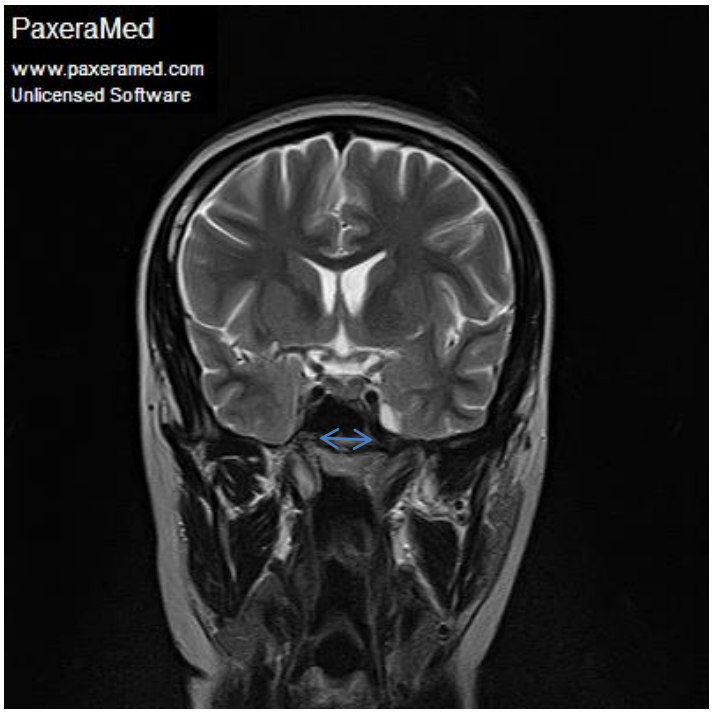

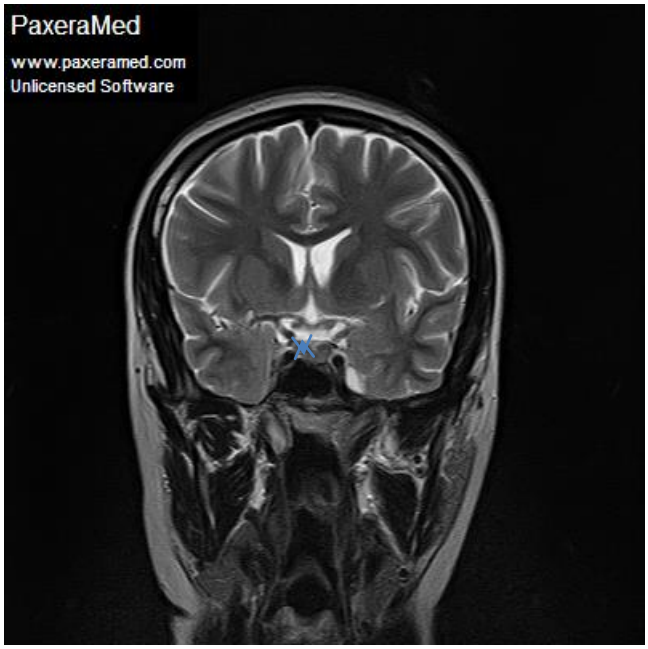

Case(14) coronal T2female/age:19years/optic chiasm width:mm14.04mm/optic chiasm height:2.46mm/finding: normal

Case(15) coronal T2,male/age:28years/optic chiasm width: 14.01mm/optic chiasm height: 2.45mm/finding: normal

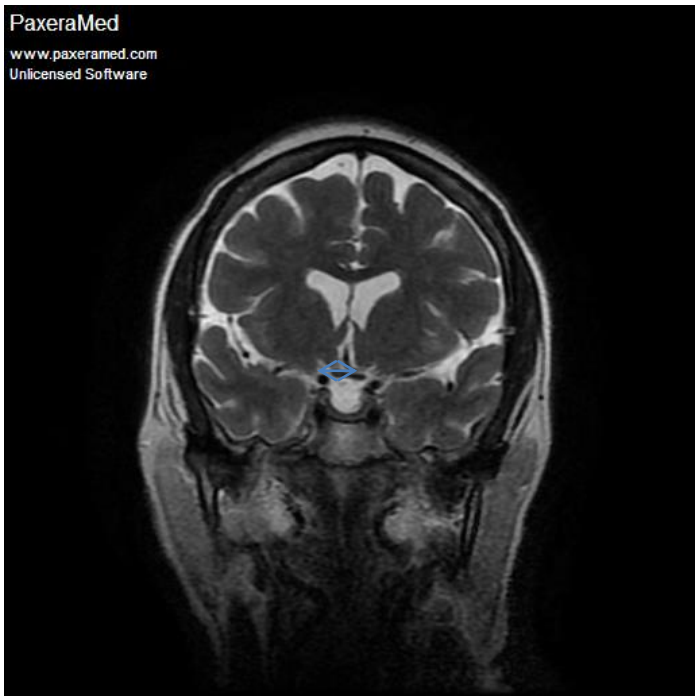

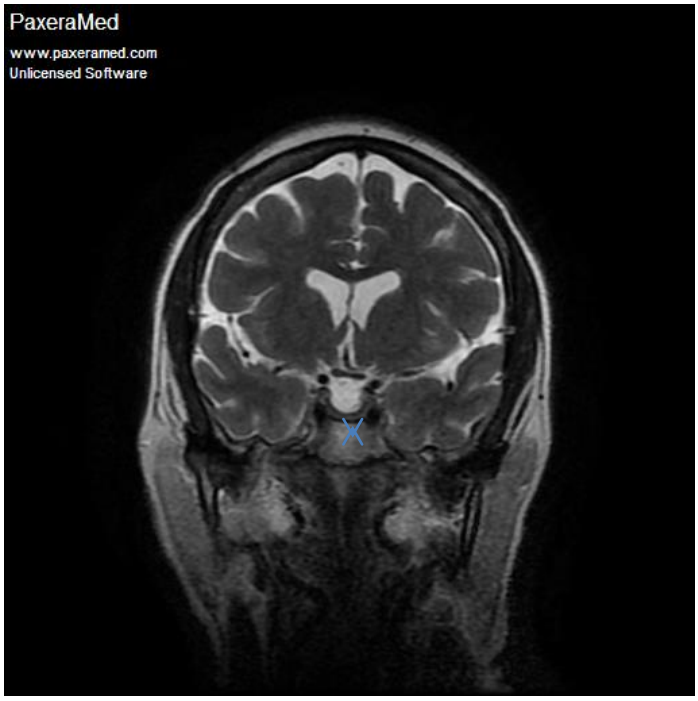

Case(16) coronal T2.female/age:56years/optic chiasm width:11.24mm/optic chiasm height:2.80mm/finding: normal

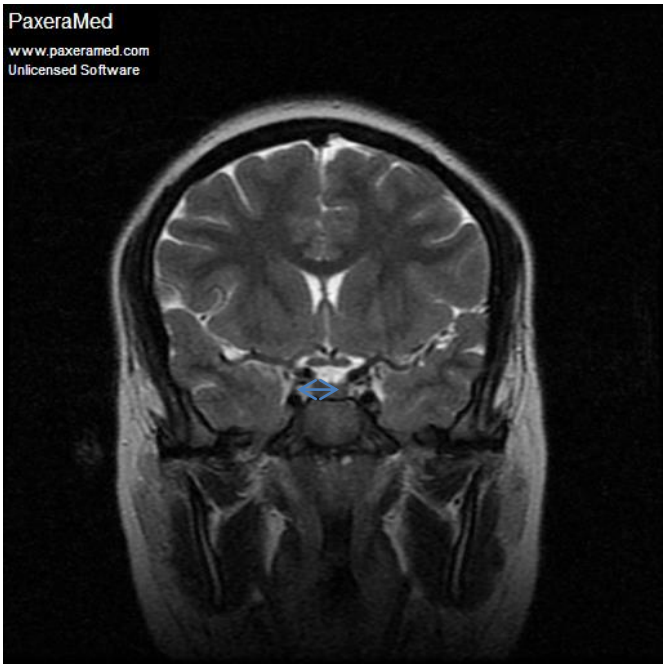

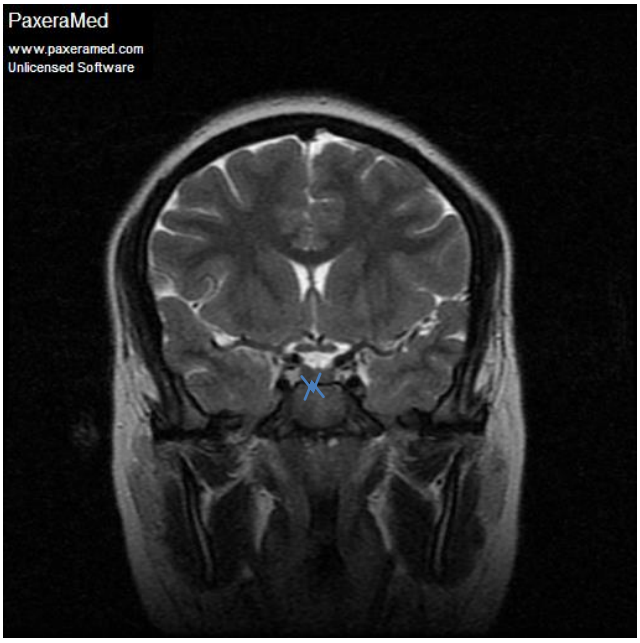

Case(17) coronal T2,female/age:20years/optic chiasm width:14.43 mm/optic chiasm height: 2.59mm/finding: normal

Appendix C Published papers:

- Bilal D, Yousef M, Abukonna A, Bushara L, Salih M. Normative Optic Chiasm Measurements Using Magnetic Resonance Imaging. Nat Sci 2018;16(9):94-98]. ISSN 1545-0740 (print); ISSN 2375-7167 (online).

  http://www.sciencepub.net/nature. 13. doi:10.7537/marsnsj160918.13.

- Dalia Bilal1" Assessment of Optic Chiasm Measurements in Abnormal MRI Brain."IOSR Journal of Dental and Medical Sciences (IOSR-JDMS), vol. 17, no. 7, 2018, pp 50-56.

  www.iosrjournals.org